

# XMM-Newton observations of the Small Magellanic Cloud: Be/X-ray binary pulsars active between October 2006 and June 2007 <sup>★</sup>

F. Haberl, P. Eger, and W. Pietsch

Max-Planck-Institut für extraterrestrische Physik, Giessenbachstraße, 85748 Garching, Germany  
e-mail: fwh@mpe.mpg.de

Received 30 April 2008 / Accepted 25 June 2008

## ABSTRACT

*Aims.* We analysed eight XMM-Newton observations toward the Small Magellanic Cloud (SMC), performed between October 2006 and June 2007, to investigate high mass X-ray binary systems.

*Methods.* We produced images from the European Photon Imaging Cameras (EPIC) and extracted X-ray spectra and light curves in different energy bands from sources which yielded a sufficiently high number of counts for a detailed temporal and spectral analysis. To search for periodicity we applied Fourier transformations and folding techniques and determined pulse periods using a Bayesian approach. To identify optical counterparts we produced X-ray source lists for each observation using maximum likelihood source detection techniques and correlated them with optical catalogues. The correlations were also used for astrometric boresight corrections of the X-ray source positions.

*Results.* We found new X-ray binary pulsars with periods of 202 s (XMMU J005929.0-723703), 342 s (XMMU J005403.8-722632), 645 s (XMMU J005535.2-722906) and 325 s (XMMU J005252.1-721715), in the latter case confirming the independent discovery in Chandra data. In addition we detected sixteen known Be/X-ray binary pulsars and six ROSAT-classified candidate high mass X-ray binaries. From one of the candidates, RX J0058.2-7231, we discovered X-ray pulsations with a period of 291 s which makes it the likely counterpart of XTE J0051-727. From the known pulsars, we revise the pulse period of CXOU J010206.6-714115 to 967 s, and we detected the 18.37 s pulsar XTE J0055-727 (= XMM J004911.4-724939) in outburst, which allowed us to localise the source. The pulse profiles of the X-ray pulsars show a large variety of shapes from smooth to highly structured patterns and differing energy dependence. For all the candidate high mass X-ray binaries optical counterparts can be identified with magnitudes and colours consistent with Be stars. Twenty of the Be/X-ray binaries were detected with X-ray luminosities in the range  $1.5 \times 10^{35}$  erg s<sup>-1</sup> -  $5.5 \times 10^{36}$  erg s<sup>-1</sup>. The majority of the spectra is well represented by an absorbed power-law with an average power-law index of 0.93. The absorption (in addition to the Galactic foreground value) varies over a wide range between a few  $10^{20}$  cm<sup>-2</sup> and several  $10^{22}$  cm<sup>-2</sup>. An overall correlation of the absorption with the total SMC HI column density suggests that the absorption seen in the X-ray spectra is often largely caused by interstellar gas.

**Key words.** galaxies: individual: Small Magellanic Cloud – galaxies: stellar content – stars: emission-line, Be – stars: neutron – X-rays: binaries

## 1. Introduction

Together with the Milky Way, the Small Magellanic Cloud (SMC) is the galaxy with the highest number of known high mass X-ray binaries (HMXBs). In these systems a compact object is accreting mass from an early type companion star. With only one exception (the supergiant system SMC X-1), the vast majority of HMXBs in the SMC comprises systems with a Be star as mass donor and a neutron star as compact object that is usually recognised as an X-ray pulsar. Depending on the eccentricity of the binary orbit, the mass accretion rate can be enhanced around the time of periastron passage when the neutron star approaches the circumstellar disc of the Be star (see, e.g., Okazaki & Negueruela 2001). These outbursts usually last a few days. Longer outbursts with durations of weeks (type II) can be caused by a drastic expansion of the disc around the Be star.

Many of the Be/X-ray binaries in the SMC were discovered during X-ray outburst. Then pulsations could be found as periodic modulation of the X-ray flux. During quiescence the sources were often not detected at all. It is not clear how many of these X-ray transients we are still missing, but present day X-ray observations with Chandra, the Rossi X-ray Timing Explorer (RXTE) and XMM-Newton keep finding new Be/X-ray binaries in the SMC with a rate of a few per year. Currently, in the SMC nearly 50 Be/X-ray binary pulsars are known (Haberl & Pietsch 2004; Coe et al. 2005). In addition, more than two dozen Be/X-ray binary candidates are discussed in the literature which are either classified as such from their X-ray properties and/or are optically identified with a Be star counterpart. In these cases, however, uncertain X-ray positions and missing X-ray pulsations make the cases less clear.

We used the European Photon Imaging Cameras (EPIC) on XMM-Newton to investigate HMXBs in the SMC. Here we report on results from eight observations - seven from our own dedicated programs to investigate candidate HMXBs and super-soft X-ray sources and one from the public archive - which cover

<sup>★</sup> Based on observations with XMM-Newton, an ESA Science Mission with instruments and contributions directly funded by ESA Member states and the USA (NASA).

**Table 1.** XMM-Newton EPIC observations of SMC fields in 2006/2007.

Observation ID	Pointing direction		Sat. Rev.	EPIC <sup>(a)</sup> Instrument configuration	Start time (UT)	End time (UT)
	R.A. (J2000.0)	Dec.				
0404680101	00 47 36.0	-73 08 24	1249	PN FF thin M1/M2 FF medium	2006-10-05 00:44:47 00:22:05	2006-10-05 06:51:09 06:50:54
0404680201	00 52 26.4	-72 52 12	1263	PN FF thin M1/M2 FF medium	2006-11-01 01:18:41 00:55:59	2006-11-01 09:58:46 09:58:31
0403970301	00 47 39.4	-72 59 31	1329	PN EFF thin M1/M2 FF thin	2007-03-12 21:02:47 20:01:50	2007-03-13 06:53:05 06:52:50
0404680301	00 51 00.7	-73 24 17	1344	PN FF thin M1/M2 FF medium	2007-04-11 20:00:39 19:37:57	2007-04-12 02:15:32 02:15:17
0404680501	01 07 42.3	-72 30 11	1344	PN FF thin M1/M2 FF medium	2007-04-12 03:29:37 03:06:55	2007-04-12 09:44:42 09:44:27
0501470101	00 59 41.8	-71:38:15	1371	PN FF thin M1/M2 FF thin	2007-06-04 09:22:05 08:59:23	2007-06-04 18:20:14 18:19:59
0500980201	01 00 00.0	-72 27 00	1372	PN FF thin M1/M2 FF medium	2007-06-06 09:14:26 08:51:44	2007-06-06 16:52:51 16:52:36
0500980101	00 53 02.4	-72 26 17	1380	PN FF thin M1/M2 FF medium	2007-06-23 06:13:53 05:51:11	2007-06-23 13:03:10 13:02:55

<sup>(a)</sup> FF: full frame CCD readout mode with 73 ms frame time for PN and 2.6 s for MOS; EFF: PN ‘extended FF’ with 200 ms frame time; thin and medium optical blocking filters.

six candidate Be/X-ray binaries and sixteen known Be/X-ray binary pulsars. We present a temporal and spectral analysis of the majority of these objects and additional newly discovered Be/X-ray binary pulsars in the SMC.

## 2. Observations and data analysis

The eight SMC fields were observed with XMM-Newton (Jansen et al. 2001) between October 2006 and June 2007. Details of the observations (in chronological order) are summarised in Table 1. The EPIC-MOS (Turner et al. 2001) and EPIC-PN (Strüder et al. 2001) cameras were operated in imaging mode, covering an area with about 28′ in diameter. The locations of the fields are superimposed on an HI image of the SMC in Fig. 1. Our dedicated observations cover part of the main bar of the SMC where most of the HMXBs are found. The archival field 0403970301, pointed at the emission nebula N19, overlaps largely with field 0404680101 (shifted by about 9′ to the north). Observation 0501470101 is part of our programme to observe supersoft X-ray sources in the SMC (Kahabka & Haberl 2006). The field is located in the north, outside the main bar of the SMC.

For the X-ray analysis we applied the same procedures as outlined in Haberl & Pietsch (2008a) and Haberl & Pietsch (2008b) using the XMM-Newton Science Analysis System (SAS) version 7.1.0 together with tools from the FTOOLS package. To be most sensitive to faint sources, intervals with increased background flaring activity were removed from our source detection analysis (standard SAS maximum likelihood method). X-ray source lists were produced for each observation and astrometric boresight corrections were applied using the optical catalogue of Zaritsky et al. (2002) as reference system. In this way we could reduce the systematic  $1\sigma$  uncertainty of the positions to  $1.1''$ .

The X-ray source lists were correlated with optical catalogues. We selected HMXB candidates using X-ray colours (hardness ratios) and the optical brightness and colours of likely optical counterparts. The resulting HMXB candidate list comprises sixteen known Be/X-ray binary pulsars (see recent compilations in Haberl & Sasaki 2000; Haberl & Pietsch 2004;

Coe et al. 2005), six candidate Be/X-ray binaries as classified in previous work (see Haberl & Sasaki 2000; Haberl & Pietsch 2004) and four new candidates, i.e. in total we selected twenty-six X-ray sources for further investigation. The results from the new Be/X-ray binary 25.55 s pulsar were published separately (Haberl et al. 2008) and we count this source here as “known” pulsar. The X-ray positions (summarised in Table 2) with a typical accuracy of  $1''$ – $2''$  (total  $1\sigma$  error inferred from the EPIC data) allowed us to securely identify the optical counterparts. In Table 4 optical brightness and colours from different optical surveys are summarised. For completeness and easier comparison we list the values for all our investigated objects. Optical counterparts from the emission line star catalogue of Meyssonnier & Azzopardi (1993, hereafter MA93) are listed in Table 2. For the newly identified Be/X-ray binaries we extracted light curves of their optical counterparts in the I-band from the Optical Gravitational Lensing Experiment (OGLE) photometry database (Szymanski 2005; Udalski et al. 1997) and the approximate B- and R-band from the Massive Compact Halo Object project (MACHO). We applied an FFT analysis to the optical light curves (Lomb 1976; Scargle 1982) to search for periodic variations which could indicate orbital periods. For this purpose we removed the long-term variations from the optical light curves which was difficult for times of fast brightness changes. In these cases we restricted the analysis to time intervals with slow and smooth variations.

In Table 3 we list known HMXBs which were covered by our observations, but were not detected. Two of them, RX J0048.5-7302 and RX J0049.5-7310, were covered twice and detected in one observation (see Table 2). XTE J0052-725 was also covered twice, but not detected in either observation. Five other known Be/X-ray binary pulsars were covered once and not detected. However, the coarse position of one of them (XTE J0052-723 with a large uncertainty in the X-ray position derived from RXTE observations) is located near the rim of field 0500980101 and the correct position might also be outside. In Table 3 we provide  $3\sigma$  upper limits of the EPIC-PN (0.2-4.5 keV) count rate (converted to X-ray luminosity with  $4 \times 10^{33}$  erg  $s^{-1}$  per  $1 \times 10^{-3}$  cts  $s^{-1}$ , see below) for the sources with accurately known posi-

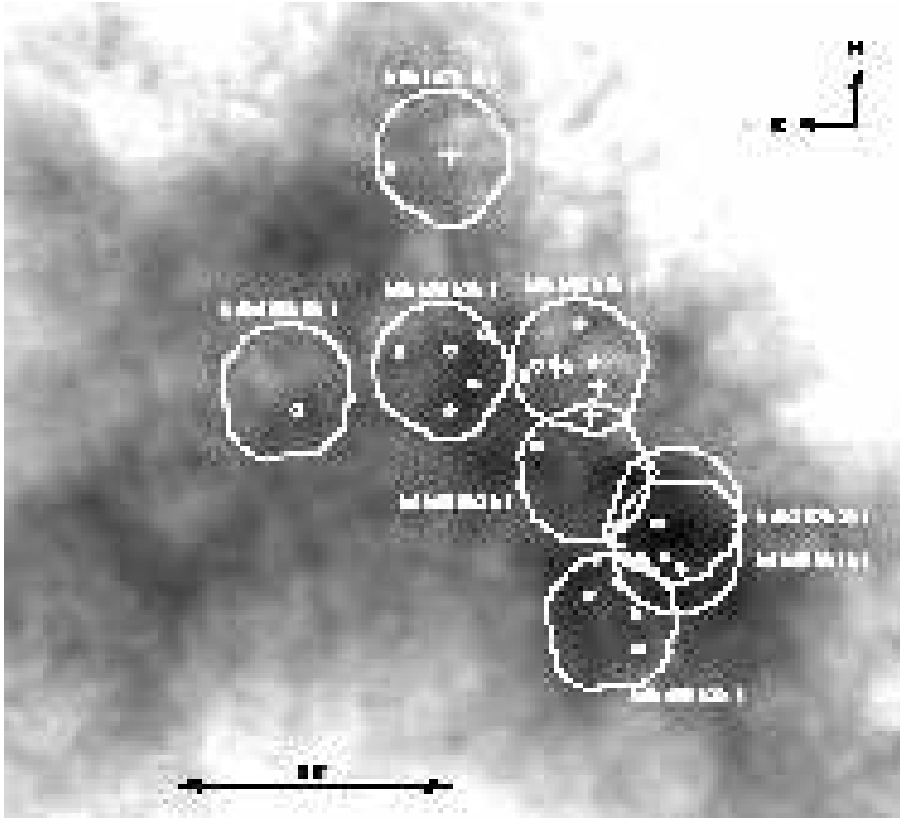


**Fig. 1.** Observed fields (marked by contours which are derived from the combined EPIC exposure maps) superimposed on an HI map of the SMC (Stanimirovic et al. 1999). The positions of the investigated Be/X-ray binaries are marked by different symbols: thin circles are used for Be/X-ray binary pulsars with previously known pulse period, thick circles indicate new discoveries from this work, boxes show the positions of Be/X-ray binaries with no detected pulse period and crosses mark the positions of known Be/X-ray binaries which we did not detect. An X-ray image of field 0500980101 is presented in Fig. 2.

tions. We mark their location in Fig. 1. We calculated the binary orbital phase of our XMM-Newton observations whenever an X-ray ephemeris from RXTE data is available for the covered pulsars (Galache et al. 2008). The phases with errors are listed in Table 2 and Table 3. Five more Be/X-ray binary candidates from correlations of ROSAT sources with emission line stars from MA93 (Haberl & Sasaki 2000) are covered by the fields. They were either not detected, or the EPIC sources found in or close to their (relatively large) ROSAT error circles are inconsistent with Be/X-ray binaries. Hence, we can not confirm nor reject their proposed Be/X-ray binary nature.

Twenty of our sources yielded a sufficient number of counts for a detailed spectral and timing analysis. For the selection of the sources we used a limit of 250 for the total number of counts (summed over the available instruments) in the 0.5–4.5 keV band as obtained by the source detection analysis. The actual counts used for the analysis differ from this value depending on the spectral shape (wider energy band used for spectral analysis) and the off-axis angle of the source. We extracted pulse-phase averaged EPIC spectra for PN (single + double pixel events, PATTERN 0–4) and MOS (PATTERN 0–12) disregarding bad CCD pixels and columns (FLAG 0) and removing intervals of increased background flaring activity. We used circular or elliptical source extraction regions depending on the off-axis angle of the source. In several cases the source extraction region was cut by bad columns or nearby CCD borders and therefore, we report fluxes and luminosities obtained from the instrument with full source extraction region. We used XSPEC version 11.3.2p for spectral modelling.

We searched for X-ray pulsations in the EPIC data (for each instrument individually and for the combined data) of each source. We created power spectra and applied folding techniques. To further investigate candidate periods and derive accurate values and errors for the detected pulse periods we used

the Bayesian method (Gregory & Loredo 1996) as described in Zavlin et al. (2000). Given period errors denote  $1\sigma$  uncertainties. For the pulsars we folded the X-ray light curves on the best period in the standard EPIC energy bands (0.2–0.5 keV, 0.5–1.0 keV, 1.0–2.0 keV, 2.0–4.5 keV, 4.5–10.0 keV and the broad band 0.2–10.0 keV) to investigate the shape and energy dependence of the pulse profiles. We fitted sine functions (with harmonics when required) to the pulse profiles in the 0.2–10.0 keV band as obtained from EPIC-PN to derive pulsed fractions. The determined pulse periods and pulsed fractions are summarised in Table 2. From the pulse profiles we computed hardness ratios as a function of pulse phase with  $HR1 = (R2-R1)/(R2+R1)$ ,  $HR2 = (R3-R2)/(R3+R2)$ ,  $HR3 = (R4-R3)/(R4+R3)$  and  $HR4 = (R5-R4)/(R5+R4)$  with  $R_i$  denoting the background-subtracted count rate in the standard band  $i$  (with energy boundaries as defined above and starting with band 1 at the lowest energies).

We present the results of our spectral analysis below. For the results on the timing analysis we refer to Sections 3, 4 and 5, where we divide the sources into Be/X-ray binaries with newly discovered pulse periods, pulsars with previously known periods and Be/X-ray binaries without detected pulse periods. Within each section the sources are sorted by field (i.e. in time) and within each field by right ascension.

We show the combined EPIC image obtained from observation 0500980101 in Fig. 2. This field is located in the central bar region, north of field 404680201 with a small overlap. In the EPIC images of this observation we detected the three known Be/X-ray binary pulsars SMC X-3 (7.79 s; Edge et al. 2004a), CXOU J005323.8-722715 (138 s; Edge et al. 2004b) and XTE J0055-724 (= 1SAX J0054.9-7226 = 1WGA J0054.9-7226 = RX J0054.9-7226, 59 s; Marshall & Lochner 1998). During this observation, three additional, previously uncatalogued X-ray sources were detected: XMMU J005252.1-721715, XMMU J005403.8-722632 and XMMU J005535.2-

**Table 2.** SMC Be/X-ray binaries detected by XMM-Newton between October 2006 and June 2007

Name	X-ray Position R.A. and Dec. (J2000.0)	Err. <sup>(a)</sup> "	MA 93	Comment <sup>(b)</sup>	Sect.	Period s	PF <sup>(d)</sup> %	Orbital Phase <sup>(e)</sup>
Observation ID 0404680101								
XMMU J004723.7-731226	00 47 23.42 –73 12 27.3	0.25	172	263 s XP	4.1	262.23±0.66	22±9	–
XMMU J004814.1-731003	00 48 14.10 –73 10 04.0	0.45	–	25.5 s XP (1)	4.2	25.550±0.002	45±15	–
RX J0049.2-7311	00 49 13.60 –73 11 36.8	0.55	–	(2)	5.2	–	–	–
RX J0049.5-7310	00 49 29.92 –73 10 59.2	0.81	300	(2)	5.2	–	–	–
Observation ID 0404680201								
CXOU J005455.6-724510	00 54 55.91 –72 45 10.6	0.49	809	500 s XP	4.3	497.5±1.0	39±16	0.00±0.04
Observation ID 0403970301								
XMMU J004723.7-731226	00 47 23.43 –73 12 27.2	0.35	172	263 s XP	4.1	<sup>(c)</sup>	–	–
XMMU J004814.1-731003	00 48 14.41 –73 10 04.6	0.91	–	25.5 s XP (1)	4.2	–	–	–
RX J0048.5-7302	00 48 34.15 –73 02 31.0	1.08	238	(2)	5.1	–	–	–
AX J0049-729	00 49 03.29 –72 50 51.9	0.53	–	74.7 s XP	4.4	–	–	0.08±0.15
XMMU J004911.4-724939	00 49 11.54 –72 49 37.3	0.08	–	18.37 s XP	4.5	18.3814±0.0001	21±3	0.97±0.11
RX J0049.2-7311	00 49 14.12 –73 11 35.8	0.49	–	(2)	5.2	–	–	–
Observation ID 0404680301								
RX J0049.5-7331	00 49 30.59 –73 31 09.1	0.33	302	(2)	5.3	–	–	–
RX J0049.7-7323	00 49 42.02 –73 23 14.5	0.23	315	755 s XP	4.6	746.15±0.79	25±5	0.14±0.10
RX J0050.8-7316	00 50 44.70 –73 16 05.1	0.18	387	323 s XP	4.7	317.44±0.26	31±7	0.00±0.11
AX J0051.6-7311	00 51 51.91 –73 10 32.6	0.59	504	172 s XP	4.8	–	–	–
RX J0052.1-7319	00 52 15.30 –73 19 14.6	0.82	–	15.3 s XP	4.9	–	–	–
Observation ID 0404680501								
CXOU J010712.6-723533	01 07 12.81 –72 35 33.1	0.22	1619	65.8 s XP	4.10	65.95±0.02	31±9	–
Observation ID 0501470101								
CXOU J010206.6-714115	01 02 06.68 –71 41 16.1	0.17	1301	967 s XP	3.1	966.97±0.47	32±17	–
Observation ID 0500980201								
CXOU J005736.2-721934	00 57 35.84 –72 19 34.2	1.14	1020	565 s XP	4.11	–	–	0.43±0.18
RX J0058.2-7231	00 58 12.64 –72 30 48.0	0.20	–	(2), 291 s XP	3.2	291.327±0.057	17±6	–
RX J0059.3-7223	00 59 21.02 –72 23 16.8	0.14	–	202 s XP	4.12	200.50±0.29	19±6	–
XMMU J005929.0-723703	00 59 29.05 –72 37 03.2	0.08	1147	NXT, 202 s XP	3.3	202.52±0.02	12.4±0.1	–
RX J0101.8-7223	01 01 52.34 –72 23 32.6	0.19	1288	(2)	5.4	–	–	–
Observation ID 0500980101								
SMC X-3	00 52 05.68 –72 26 05.3	0.14	531	7.78 s XP	4.13	7.7912±0.0096	18±6	0.05±0.09
XMMU J005252.1-721715	00 52 52.12 –72 17 15.7	0.21	–	NXT, 325 s XP	3.4	325.36±0.59	20±7	–
CXOU J005323.8-722715	00 53 23.97 –72 27 15.3	0.16	667	138 s XP	4.14	139.136±0.016	42±8	0.09±0.14
XMMU J005403.8-722632	00 54 03.88 –72 26 32.8	0.27	–	NXT, 342 s XP	3.5	341.87±0.15	54±12	–
XTE J0055-724	00 54 56.20 –72 26 47.1	0.36	810	59 s XP	4.15	58.858±0.001	90±23	0.12±0.08
XMMU J005535.2-722906	00 55 35.24 –72 29 06.2	0.19	–	NXT, 645 s XP	3.6	644.55±0.72	14±14	–

<sup>(a)</sup> Statistical 1 $\sigma$  uncertainty, the systematic error is 1.1".<sup>(b)</sup> NXT: New Be/X-ray transient; XP: X-ray pulsar References: (1) published separately in Haberl et al. (2008), (2) candidate BeX from Haberl & Sasaki (2000).<sup>(c)</sup> Although sufficient number of counts, pulsations not detected (see text).<sup>(d)</sup> Pulsed fraction obtained from 0.2-10.0 keV EPIC-PN pulse profiles.<sup>(e)</sup> Orbital phase calculated from the X-ray ephemeris listed in Galache et al. (2008).

722906. All three exhibit X-ray spectra typical for high mass X-ray binaries and their optical counterparts are consistent with Be stars. Moreover, we detect X-ray pulsations from all three, clearly identifying them as Be/X-ray binary pulsars. Thus, from the ten brightest sources detected in this field six are Be/X-ray binary pulsars. The other four are most likely active galactic nuclei (AGN) due to their steeper power-law X-ray spectra and faint optical counterparts. One of them is listed as HMXB candidate (SMC 36 in Shtykovskiy & Gilfanov 2005) from XMM-Newton data. However, our new observation yielded a factor of four more counts from this source and we obtain a spectral index of  $1.5\pm 0.2$ , probably too steep for a HMXB.

For each source, the EPIC spectra (in some cases MOS spectra are not available) were simultaneously fit with a power-law model (which in most cases yields acceptable fits) allowing for a normalization factor between the spectra from different cameras. We included two absorption components in our spectral model, accounting for the Galactic foreground absorption (with a fixed hydrogen column density of  $6\times 10^{20}$  cm<sup>-2</sup> and with elemental abundances from Wilms et al. 2000) and the SMC absorption (with column density as free parameter in the fit and with metal abundances reduced to 0.2 as typical for the SMC; Russell & Dopita 1992).

For twenty sources (adding the results for XMMU J004814.1-731003 from Haberl et al. 2008) the

**Table 3.** SMC high mass X-ray binaries not detected by XMM-Newton.

Observation ID	Name	Upper limit $10^{-3}$ cts $s^{-1}$ / $10^{34}$ erg $s^{-1}$	Orbital Phase	Comment Comment
0404680101	RX J0048.5-7302	13.1 / 5.2	–	no pulsations found yet, see also detection in 0403970301
0404680201	XTE J0052-725	7.9 / 3.2	$0.39 \pm 0.07$	82.4 s pulsar (Corbet et al. 2002)
0403970301	RX J0049.5-7310	11.9 / 4.8	–	no pulsations found yet, see also detection in 0404680101
0501470101	RX J0059.2-7138	7.5 / 3.0	–	2.76 s pulsar (Hughes 1994)
0500980101	RX J0051.8-7231	6.0 / 2.4	$0.11 \pm 0.12$	8.9 s pulsar (Israel et al. 1997)
	XTE J0052-725	8.9 / 3.6	$0.03 \pm 0.08$	82.4 s pulsar (Corbet et al. 2002)
	XTE J0052-723	–	–	4.78 s pulsar (Laycock et al. 2003) uncertain position
	XTE J0053-724	4.2 / 1.7	$0.42 \pm 0.05$	46.6 s pulsar (Corbet et al. 1998)

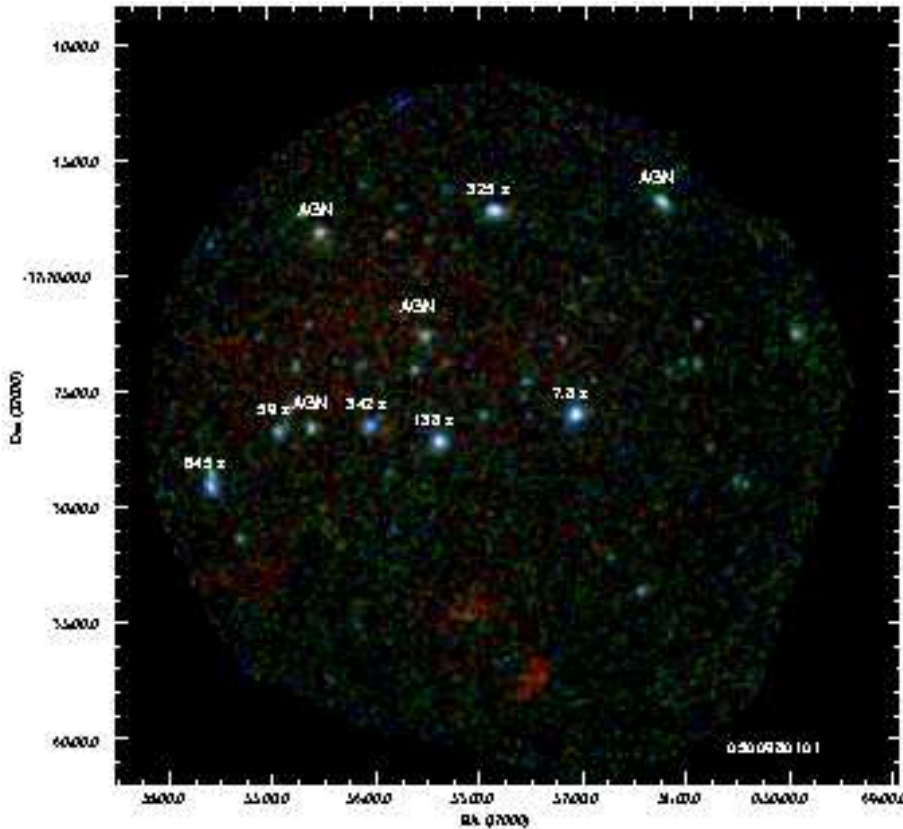


**Fig. 2.** EPIC RGB colour image of the field 0500980101, composed of images from the three energy bands 0.2–1.0 keV (red), 1.0–2.0 keV (green) and 2.0–4.5 keV (blue) and from all three EPIC instruments. The individual images are exposure corrected and EPIC-PN out-of-time events are subtracted. The ten brightest X-ray sources in the image are marked, the Be/X-ray binary pulsars by their pulse periods. Four likely AGN exhibit power-law X-ray spectra steeper than those of HMXBs. They appear less blue in the colour representation of the image. The southern of the two patches of diffuse emission seen in the lower part of the image is related to a supernova remnant (SNR B0050-72.8) known from radio and optical wavelengths, the other one might also be a SNR, however, without radio and optical emission (Filipović et al. 2008).

derived best fit parameters for the power-law model together with observed fluxes and source luminosities are summarised in Table 5. The table also lists net exposure times for each EPIC instrument. Example spectra together with their best fit model are plotted in Fig. 3. To estimate luminosities for the detected sources which did not yield a sufficient number of counts for a spectrum, we converted the count rates, obtained by the source detection analysis, assuming an appropriate spectral shape (using spectral parameters from the same source from a different observation when available or from a nearby Be/X-ray binary to at least get an estimate for the absorbing column density; see below and the sections on the individual sources). The luminosities are listed in Table 5 and more details can be found in the description of each individual source in the next sections.

### 3. New Be/X-ray binary pulsars

In this section we present the results of our analysis of the new pulsars. This includes CXOU J010206.6-714115 for which we revise the period; RX J0058.2-7231, a former candidate Be/X-ray binary known from ROSAT; the new transient XMMU J005929.0-723703 which is the second 202 s pulsar in the SMC (both are only 13.8' apart); and the three previously unknown sources XMMU J005252.1-721715, XMMU J005403.8-722632 and XMMU J005535.2-722906 which were discovered in field 0500980101.

#### 3.1. A revised period of 967 s for the Be/X-ray binary pulsar CXOU J010206.6-714115

We included observation 0501470101 into our analysis to investigate the X-ray properties of CXOU J010206.6-714115 for

**Table 4.** Optical identifications (continued next page).

Source	Catalogue <sup>(a)</sup>	R.A. and Dec. (J2000.0)	Vmag	B-V	U-B	V-R	V-I
XMMU J004723.7-731226	UBVR	00 47 23.97 -73 12 25.9	14.37 <sup>(b)</sup>	-0.06	-0.83	+0.05	-
	MCPS	00 47 23.42 -73 12 27.3	16.03	+0.08	-0.97	-	+0.05
	OGLE	00 47 23.35 -73 12 27.0	16.14	-0.04	-	-	+0.14
XMMU J004814.1-731003	UBVR	00 48 14.10 -73 10 04.0	15.25	+0.13	-0.64	+0.12	-
	MCPS	00 48 14.18 -73 10 03.9	15.30	+0.26	-0.50	-	-0.21
	OGLE	00 48 14.13 -73 10 03.5	15.71	+0.01	-	-	+0.09
RX J0049.2-7311	UBVR	00 49 13.59 -73 11 37.0	15.67	+0.25	-0.71	+0.19	-
	MCPS	00 49 13.68 -73 11 37.5	16.44	+0.19	-0.92	-	+0.16
	OGLE	00 49 13.63 -73 11 37.4	16.51	+0.10	-	-	+0.30
RX J0049.5-7310	UBVR	00 49 29.78 -73 10 58.7	15.66	+0.19	-0.49	+0.28	-
	MCPS	00 49 29.87 -73 10 58.2	16.15	+0.20	-0.88	-	+0.14
	OGLE	00 49 29.81 -73 10 58.0	16.30	+0.09	-	-	+0.33
CXOU J005455.6-724510	UBVR	00 54 55.88 -72 45 10.5	14.78	-0.05	-0.90	+0.05	-
	MCPS	00 54 55.91 -72 45 10.5	15.00	-0.03	-0.93	-	+0.10
	OGLE	00 54 55.87 -72 45 10.7	14.99	-0.02	-	-	+0.20
RX J0048.5-7302	UBVR	00 48 34.08 -73 02 31.1	14.84	-0.05	-0.79	+0.18	-
	MCPS	00 48 34.17 -73 02 30.8	14.78	+0.00	-0.81	-	+0.02
	OGLE	00 48 34.12 -73 02 30.9	15.06	-0.23	-	-	+0.31
AX J0049-729	UBVR	00 49 03.35 -72 50 52.0	16.09	+0.12	-0.59	+0.12	-
	MCPS	00 49 03.41 -72 50 52.3	16.78	+0.08	-0.84	-	+0.17
	OGLE	00 49 03.34 -72 50 52.1	16.92	+0.09	-	-	+0.24
XMMU J004911.4-724939	UBVR	00 49 11.40 -72 49 37.2	15.61	+0.19	-0.64	+0.19	-
	MCPS	00 49 11.53 -72 49 37.2	15.96	+0.05	-0.79	-	+0.07
	OGLE	00 49 11.45 -72 49 37.1	15.71	+0.07	-	-	+0.21
RX J0049.5-7331	UBVR	00 49 30.39 -73 31 10.2	13.83 <sup>(b)</sup>	-0.04	-0.92	-0.89	-
	MCPS	00 49 30.55 -73 31 09.1	14.64	-0.04	-0.86	-	+0.09
	OGLE	00 49 30.53 -73 31 08.8	14.66	-0.06	-	-	+0.16
RX J0049.7-7323	UBVR	00 49 41.99 -73 23 14.6	14.86	+0.04	-0.86	-0.89	-
	MCPS	00 49 42.03 -73 23 14.4	14.86	+0.15	-0.91	-	+0.16
	OGLE	00 49 42.02 -73 23 14.2	14.98	+0.05	-	-	+0.25
RX J0050.8-7316	UBVR	00 50 44.66 -73 16 05.4	15.25	-0.03	-0.94	+0.07	-
	MCPS	00 50 44.75 -73 16 05.3	15.48	-0.11	-0.91	-	+0.17
	OGLE	00 50 44.71 -73 16 05.0	15.44	-0.04	-	-	+0.17
AX J0051.6-7311	UBVR	00 51 52.01 -73 10 33.8	14.33	-0.04	-0.94	+0.09	-
	MCPS	00 51 52.08 -73 10 33.9	14.45	-0.07	-0.99	-	+0.16
	OGLE	00 51 52.02 -73 10 33.6	14.45	-0.07	-	-	+0.09
RX J0052.1-7319	MCPS	00 52 15.48 -73 19 15.1	15.90	-0.14	-0.95	-	-0.20
	OGLE	00 52 15.39 -73 19 15.0	15.91	-0.10	-	-	-0.03
CXOU J010712.6-723533	UBVR	01 07 12.58 -72 35 33.6	15.64	-0.12	-0.75	-0.12	-
	MCPS	01 07 12.58 -72 35 33.3	15.64	-0.09	-0.83	-	-0.09
	OGLE	01 07 12.59 -72 35 33.5	15.76	-0.14	-	-	+0.00
CXOU J010206.6-714115	UBVR	01 02 06.65 -71 41 15.9	14.56	-0.08	-1.12	-1.06	-
	MCPS	01 02 06.68 -71 41 16.1	14.37	+0.21	-1.04	-	-0.05
CXOU J005736.2-721934	UBVR	00 57 36.06 -72 19 33.8	15.84	-0.10	-0.85	+0.05	-
	MCPS	00 57 36.09 -72 19 33.6	15.99	+0.01	-1.06	-	+0.19
	OGLE	00 57 36.01 -72 19 33.8	15.97	-0.02	-	-	+0.26
RX J0058.2-7231	UBVR	00 58 12.65 -72 30 48.5	14.78	+0.06	-0.91	-0.95	-
	MCPS	00 58 12.63 -72 30 48.2	14.87	+0.11	-1.07	-	+0.26
	OGLE	00 58 12.58 -72 30 48.5	14.89	+0.06	-	-	+0.27
RX J0059.3-7223	UBVR	00 59 21.10 -72 23 17.2	14.65	-0.06	-0.92	-0.88	-
	MCPS	00 59 21.04 -72 23 16.7	14.98	-0.01	-1.16	-	-0.10
	OGLE	00 59 21.04 -72 23 17.0	14.83	-0.07	-	-	+0.03
XMMU J005929.0-723703	UBVR	00 59 28.75 -72 37 04.1	15.31	+0.01	-0.77	+0.16	-
	MCPS	00 59 28.70 -72 37 04.2	15.53	+0.05	-1.01	-	+0.20
	OGLE	00 59 28.67 -72 37 03.9	15.60	-0.03	-	-	+0.21
RX J0101.8-7223	UBVR	01 01 52.21 -72 23 34.1	14.61	-0.04	-0.90	-0.87	-
	MCPS	01 01 52.25 -72 23 33.8	14.94	-0.01	-1.09	-	+0.09
	OGLE	01 01 52.28 -72 23 33.7	14.98	-0.06	-	-	+0.14

**Table 4.** Continued.

Source	Catalogue	R.A. and Dec. (J2000.0)	Vmag	B-V	U-B	V-R	V-I
SMC X-3	UBVR	00 52 05.67 -72 26 04.0	14.94	-0.09	-0.99	+0.03	-
	MCPS	00 52 05.69 -72 26 03.9	14.91	-0.00	-0.97	-	+0.08
XMMU J005252.1-721715	UBVR	00 52 52.21 -72 17 15.0	16.33	-0.09	-0.35	-0.10	-
	MCPS	00 52 52.26 -72 17 14.7	16.62	-0.21	-0.58	-	-0.2
CXOU J005323.8-722715	UBVR	00 53 23.78 -72 27 15.4	16.04	-0.06	-0.92	+0.17	-
	MCPS	00 53 23.90 -72 27 15.4	16.19	-0.09	-1.05	-	+0.05
XMMU J005403.8-722632	UBVR	00 54 03.81 -72 26 33.0	14.81	-0.04	-0.90	+0.01	-
	MCPS	00 54 03.92 -72 26 32.8	14.94	+0.01	-1.13	-	+0.15
XTE J0055-724	UBVR	00 54 56.13 -72 26 48.1	14.39 <sup>(b)</sup>	-0.11	-0.79	+0.00	-
	MCPS	00 54 56.26 -72 26 47.4	15.27	-0.05	-1.07	-	+0.16
XMMU J005535.2-722906	OGLE	00 54 56.17 -72 26 47.6	15.28	-0.04	-	-	+0.15
	UBVR	00 55 35.21 -72 29 06.5	14.36	-0.01	-0.87	+0.15	-
	MCPS	00 55 35.20 -72 29 06.1	14.69	-0.04	-1.05	-	+0.01
	OGLE	00 55 35.13 -72 29 06.4	14.69	-0.05	-	-	+0.11

<sup>(a)</sup> From the UBVR CCD Survey (Massey 2002), the Magellanic Clouds Photometric Survey (MCPS, Zaritsky et al. 2002) and the Optical Gravitational Lensing Experiment (OGLE) BVI photometry catalogue (Udalski et al. 1998) <sup>(b)</sup> Blend of stars.

**Table 5.** Spectral fit results for the power-law model.

Source	SMC N <sub>H</sub> [10 <sup>21</sup> cm <sup>-2</sup> ]	Photon Index	Flux <sup>(a)</sup> erg cm <sup>-2</sup> s <sup>-1</sup>	L <sub>x</sub> <sup>(b)</sup> erg s <sup>-1</sup>	$\chi^2_r$ /dof	Net exposure time (s)			SMC N <sub>H</sub> <sup>(c)</sup> [10 <sup>21</sup> cm <sup>-2</sup> ]
						PN	MOS1	MOS2	
XMMU J004723.7-731226	7.4 <sup>+2.4</sup> <sub>-1.0</sub>	0.97 <sup>+0.05</sup> <sub>-0.10</sub>	7.8×10 <sup>-13</sup>	3.7×10 <sup>35</sup>	0.82/110	16550	18498	18508	9.6
XMMU J004814.1-731003 <sup>(d)</sup>	52±20	1.33±0.27	3.5×10 <sup>-13</sup>	2.1×10 <sup>35</sup>	0.82/27	19044	22760	22772	10.8
RX J0049.2-7311	13 <sup>+14</sup> <sub>-8</sub>	0.96 <sup>+0.34</sup> <sub>-0.23</sub>	3.4×10 <sup>-13</sup>	1.7×10 <sup>35</sup>	1.08/41	16563	-	18520	10.6
RX J0049.5-7310	9.4 <sup>+6.9</sup> <sub>-4.4</sub>	0.83 <sup>+0.24</sup> <sub>-0.21</sub>	4.3×10 <sup>-13</sup>	2.0×10 <sup>35</sup>	0.58/23	16563	-	18520	10.4
CXOU J005455.6-724510	6.2 <sup>+4.5</sup> <sub>-1.2</sub>	0.85 <sup>+0.30</sup> <sub>-0.14</sub>	2.9×10 <sup>-13</sup>	1.3×10 <sup>35</sup>	1.20/15	27174	30324	30365	6.8
XMMU J004723.7-731226	5.6 <sup>+3.8</sup> <sub>-2.5</sub>	1.00±0.17	7.8×10 <sup>-13</sup>	3.7×10 <sup>35</sup>	1.13/33	17728	24785	24813	9.6
XMMU J004814.1-731003				9.1×10 <sup>33</sup>		faint			10.8
RX J0048.5-7302				1.0×10 <sup>34</sup>		faint			11.1
AX J0049-729				1.1×10 <sup>35</sup>		faint			9.4
XMMU J004911.4-724939	19.4±1.8	0.65±0.05	1.2×10 <sup>-11</sup>	5.5×10 <sup>36</sup>	1.02/364	17682	24804	24820	9.3
RX J0049.2-7311				2.2×10 <sup>34</sup>		faint			10.6
RX J0049.5-7331	0.2 <sup>+1.6</sup> <sub>-0.2</sub>	0.70 <sup>+0.16</sup> <sub>-0.13</sub>	4.0×10 <sup>-13</sup>	1.8×10 <sup>35</sup>	0.98/22	14231	17408	17458	6.6
RX J0049.7-7323	10.1 <sup>+3.0</sup> <sub>-2.4</sub>	0.92±0.11	9.6×10 <sup>-13</sup>	4.5×10 <sup>35</sup>	1.17/59	14235	-	-	7.5
RX J0050.8-7316	6.5 <sup>+2.3</sup> <sub>-0.9</sub>	0.81 <sup>+0.10</sup> <sub>-0.09</sub>	1.1×10 <sup>-12</sup>	5.3×10 <sup>35</sup>	1.22/96	14228	17414	17451	8.0
AX J0051.6-7311						at edge of FOV, faint			7.3
RX J0052.1-7319				4.0×10 <sup>34</sup>		faint			8.1
CXOU J010712.6-723533	7.1 <sup>+3.9</sup> <sub>-0.3</sub>	0.74 <sup>+0.12</sup> <sub>-0.11</sub>	1.6×10 <sup>-12</sup>	7.3×10 <sup>35</sup>	1.69/73	19121	22871	22916	6.4
CXOU J010206.6-714115	0.15 <sup>+0.47</sup> <sub>-0.15</sub>	0.71 <sup>+0.07</sup> <sub>-0.06</sub>	2.1×10 <sup>-12</sup>	9.3×10 <sup>35</sup>	0.93/135	20222	24276	24320	3.5
CXOU J005736.2-721934						at edge of FOV, faint			6.3
RX J0058.2-7231	13.5±3.2	1.27±0.12	8.3×10 <sup>-13</sup>	4.4×10 <sup>35</sup>	0.97/48	23810	28132	28198	8.3
RX J0059.3-7223	3.4±0.7	1.20±0.06	8.1×10 <sup>-13</sup>	3.9×10 <sup>35</sup>	0.78/95	23816	28203	28205	7.5
XMMU J005929.0-723703	5.4±0.5	0.90±0.03	9.6×10 <sup>-12</sup>	4.5×10 <sup>36</sup>	1.05/364	23777	28212	28256	7.6
RX J0101.8-7223	4.6±1.6	1.01±0.09	8.4×10 <sup>-13</sup>	3.9×10 <sup>35</sup>	0.94/49	23798	28163	28189	5.4
SMC X-3	5.0 <sup>+1.7</sup> <sub>-1.0</sub>	0.92±0.07	9.3×10 <sup>-13</sup>	4.3×10 <sup>35</sup>	1.49/58	20107	24016	24031	2.9
XMMU J005252.1-721715	1.4 <sup>+0.8</sup> <sub>-0.8</sub>	1.05±0.09	7.2×10 <sup>-13</sup>	3.3×10 <sup>35</sup>	1.10/31	20109	-	24034	4.0
CXOU J005323.8-722715	2.9 <sup>+1.3</sup> <sub>-0.9</sub>	0.97±0.07	6.6×10 <sup>-13</sup>	3.0×10 <sup>35</sup>	1.26/48	20101	24016	24031	4.1
XMMU J005403.8-722632	0.6 <sup>+5.5</sup> <sub>-0.6</sub>	0.37 <sup>+0.19</sup> <sub>-0.12</sub>	3.5×10 <sup>-13</sup>	1.5×10 <sup>35</sup>	1.37/26	20095	24016	24031	3.7
XTE J0055-724				9.2×10 <sup>34</sup>		faint			5.1
XMMU J005535.2-722906	2.7 <sup>+1.3</sup> <sub>-1.0</sub>	0.85 <sup>+0.10</sup> <sub>-0.09</sub>	1.1×10 <sup>-12</sup>	4.9×10 <sup>35</sup>	0.69/56	20090	24004	24050	5.3

<sup>(a)</sup> Observed 0.2-10.0 keV flux. <sup>(b)</sup> Source intrinsic X-ray luminosity in the 0.2-10.0 keV band (corrected for absorption) for a distance to the SMC of 60 kpc (Hilditch et al. 2005). <sup>(c)</sup> Total SMC HI column density from Stanimirovic et al. (1999). <sup>(d)</sup> From Haberl et al. (2008).

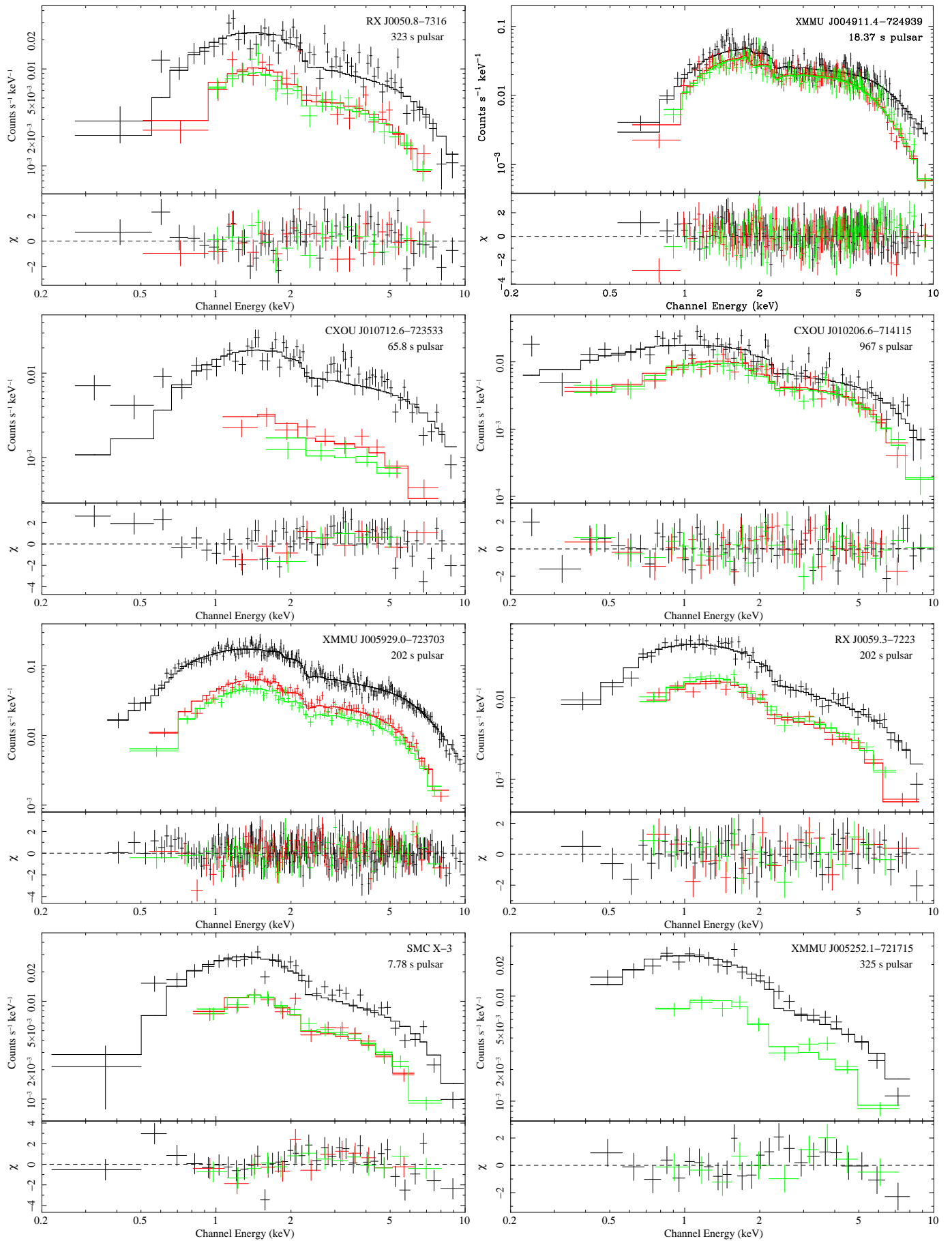


**Fig. 3.** EPIC spectra of selected Be/X-ray binaries. EPIC-PN is shown in black and EPIC-MOS in red (M1) and green (M2) (both grey in black and white representation). The histograms show the best-fit absorbed power-law model.

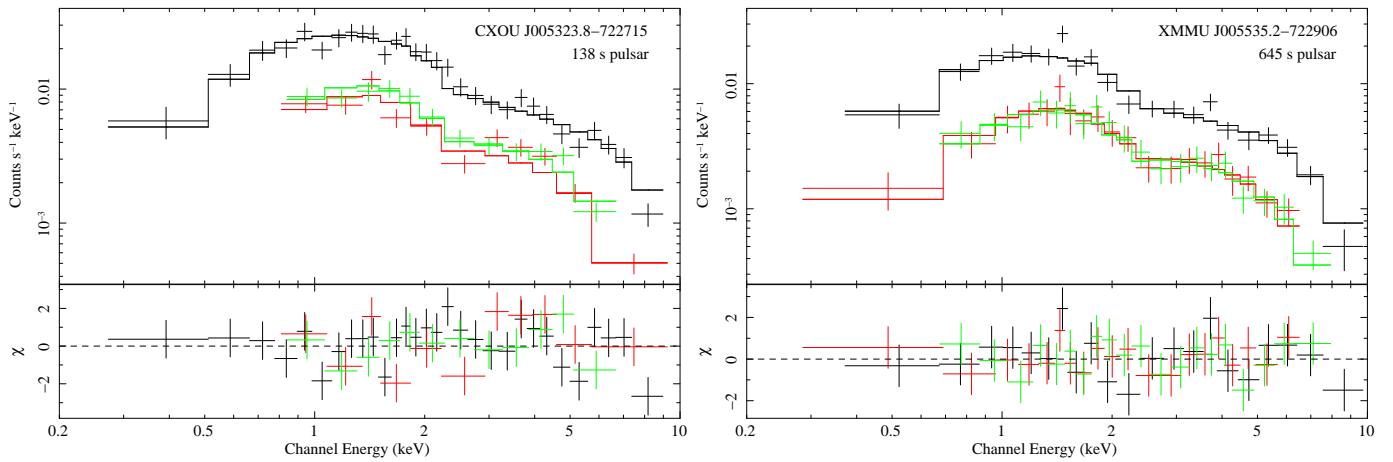


**Fig. 3.** Continued.

which a pulse period of  $700 \pm 34$  s was claimed (McGowan et al. 2007). The error on the period is large and the value is close to the Chandra dithering period of 707 s.

We detected a source in the EPIC images (the second brightest source after the supersoft source RX J0058.6-7136) within  $0.31''$  of the Chandra source. From the EPIC data we find a strong peak in the power spectrum at  $1.037 \times 10^{-3}$  Hz (Fig. 4). Bayesian analysis yields  $966.97 \pm 0.47$  s for the pulse period. Pulse profiles in the standard energy bands are presented in Fig. 5 which show a modulation with a broad peak at all energies. The X-ray spectrum shows relatively low absorption and the power-law index of 0.7 indicates a somewhat harder spectrum than the average SMC Be/X-ray binaries (Table 5, Fig. 3). The X-ray position obtained from the EPIC data coincides exactly with that of the optical star from the MCPS (Table 4) which was suggested as the optical counterpart of CXOU J010206.6-714115 (McGowan et al. 2007).

Although we can not confirm the 700 s period, reported for CXOU J010206.6-714115, it is extremely unlikely that the EPIC (observation date 2007 June 4) and Chandra (2006 Feb. 6) detections do not arise from the same source. We therefore re-analysed the Chandra data of CXOU J010206.6-714115. Using the standard level 2 event file, which is cleaned for CCD columns with higher background than adjacent columns, we produced images in detector coordinates. The images show missing columns which are crossed by the source during the dithering motion. Timing analysis based on these data reveals a period of  $\sim 700$  s. We then created a new level 2 event file that did not reject these columns (keeping all other standard screening criteria). Timing analysis of the new data does not show the periodicity at 700 s, suggesting that the period found in the standard level 2 data is caused by the satellite dithering. In the new dataset, we searched without success for the periodic signal at 967 s, found in the XMM-Newton data. This may be caused by the exposure time of 9.4 ks, which covers only less than 10 periods.

### 3.2. Discovery of 291 s pulsations from RX J0058.2-7231

The power spectrum of the combined EPIC data revealed peaks at the fundamental frequency of  $3.44 \times 10^{-3}$  Hz, at the first harmonic, which dominates in power, and at the third harmonic (Fig. 4). The resulting pulse period from the Bayesian analysis is  $291.327 \pm 0.057$  s. This period is close to the values found for XTE J0051-727, which was discovered with periods of  $293.9 \pm 0.4$  s and  $292.7 \pm 0.4$  s on 2004, April 19 and April

22, respectively (Corbet et al. 2004). The XMM-Newton position is  $32'$  away from the published RXTE position, outside the formal error box, but still inside the field of view of the PCA. XTE J0051-727 and RX J0058.2-7231 are very likely the same source. The pulsar was detected by RXTE several times in 2003 and 2004 with periods around 293 s. After the last outburst which lasted longer than one week, the period had decreased to  $\sim 291$  s (Galache et al. 2008), similar to the value measured in our XMM-Newton observation. The pulse profiles obtained from the EPIC data (Fig. 5) show a broad peak below 2.0 keV which changes to a depression at higher energies. Schmidtke et al. (1999) suggested a  $V=14.9$  mag Be star as optical counterpart for this ROSAT HRI source (source 76 in Sasaki et al. 2000). Our improved XMM-Newton position confirms the identification with this star and its optical magnitudes and colours are listed in Table 4. The spectral type was determined to B0IIIe by Mennickent et al. (2006).

### 3.3. XMMU J005929.0-723703, a new transient 202 s Be/X-ray binary pulsar

The XMM-Newton observation 0500980201 revealed a previously unreported source for which we assign the name XMMU J005929.0-723703. It was the brightest source in the field and yielded the highest number of counts from all sources in our sample. During the observation XMMU J005929.0-723703 showed strong flaring activity on timescales of an hour with intensity increases up to a factor of three. The broad band EPIC-PN light curve is shown in Fig. 6. A Fourier timing analysis of the EPIC-PN data revealed the presence of strong peaks at four harmonic frequencies with the fundamental frequency corresponding to a period of  $202.52 \pm 0.02$  s (Fig. 4).

Pulse profiles and the corresponding hardness ratio variations versus pulse phase are shown in Figs. 5 and 10. The pulse profile of XMMU J005929.0-723703 is dominated by two broad main pulses which show additional sub-structure. The shape and the relative intensity of the main pulses are energy dependent. While at energies below  $\sim 2$  keV the two main pulses are different in shape and amplitude, they become more and more similar at higher energies. This causes the highest power in the power spectrum in the first harmonic at 101 s. Significant differences in HR3 between the main pulses indicate a change in the intrinsic source spectrum during the pulse period.

From the X-ray position we identify a  $V 14.9$  Be star as optical counterpart (Table 4). This star ([MA93] 1147) is listed in

the 2dF survey of the SMC with a spectral type of B0-5(III) (Evans et al. 2004). The light curves obtained from the MACHO database show a long-term brightness increase with  $\sim 0.05$  mag variations on top of it (Fig. 7). We applied an FFT analysis to the MACHO R-band data (Lomb 1976; Scargle 1982) to look for periodicity. The power spectrum shows the strongest peaks at 334 days and 220 days (with power of 26 and 16, respectively). Although similarly long orbital periods were suggested for SMC Be/X-ray binaries (Galache et al. 2008), the broad peaks indicate more quasi-periodic variations as they might be expected from changes in the Be disk.

#### 3.4. *XMMU J005252.1-721715, a new transient 325 s Be/X-ray binary pulsar*

Three previously unreported sources were detected in the EPIC data of observation 0500980101, the first is designated XMMU J005252.1-721715. The power spectrum (Fig. 4) shows a single peak and the Bayesian analysis yields  $325.36 \pm 0.59$  s for the period. The pulse profiles (Fig. 5) reveal significant modulation mainly below 2.0 keV. The period of this pulsar is close to that of AX J0051-733 (= RX J0050.7-7316) with  $323.2 \pm 0.4$  s detected in ASCA data in November 1997 (Yokogawa & Koyama 1998b). The angular separation of the two pulsars is  $59.6'$ . During the preparation of this paper Coe et al. (2008) reported an optical and RXTE X-ray study of a new X-ray binary pulsar (period  $\sim 327$  s) based on a detection in Chandra data. The Chandra position is consistent with that of XMMU J005252.1-721715 and the similar periods confirm that the same new Be/X-ray binary pulsar was independently detected in Chandra and XMM-Newton data. For information on the optical counterpart we refer to Coe et al. (2008).

#### 3.5. *XMMU J005403.8-722632, a new transient 342 s Be/X-ray binary pulsar*

The second transient source from observation 0500980101 also shows a single peak in the power spectrum (Fig. 4). The pulse period was determined to  $341.87 \pm 0.15$  s. The pulse profile (Fig. 5) is characterised by a broad, nearly triangular-shaped peak at all energies. The pulse period of XMMU J005403.8-722632 is close to the value of SAX J0103.2-7209 ( $345.2 \pm 0.1$  s detected in BeppoSAX data of July 1998; Israel et al. 1998). The two pulsars are separated by  $45.2'$ . Galache et al. (2008) investigated the spin history of the pulsar SXP348 obtained from the RXTE SMC monitoring program. They identify this pulsar with SAX J0103.2-7209. The large scatter seen in the pulse periods may, however, be caused by the RXTE detection of two different pulsars, SAX J0103.2-7209 and our new pulsar XMMU J005403.8-722632.

As optical counterpart of XMMU J005403.8-722632 we identify a star with  $V \sim 14.9$  (Table 4) which shows large (0.7 mag, 0.5 mag) variations in the MACHO (R-band, B-band) light curves (Fig. 7). This star (entry 28942 in Massey (2002)) was also proposed as possible counterpart of an INTEGRAL source with a potential periodicity of 6.8 s (McBride et al. 2007). If this periodicity is confirmed, the star can not be the optical counterpart of the INTEGRAL source. On the other hand, if the periodicity is spurious, XMMU J005403.8-722632 might be the X-ray counterpart of the INTEGRAL source. XMMU J005403.8-722632 shows the hardest power-law X-ray spectrum of all our investigated Be/X-ray binaries in the SMC, which could explain a detection by INTEGRAL.

#### 3.6. *XMMU J005535.2-722906, a new transient 645 s Be/X-ray binary pulsar*

This source is the third transient detected in the data from observation 0500980101. The power spectrum shows peaks at the fundamental frequency and its first harmonic (Fig. 4). The pulse period is  $644.55 \pm 0.72$  s. The pulse profiles show relatively shallow modulation with broad peaks (Fig. 5). The profiles below and above 2.0 keV are nearly anti-correlated in intensity.

As optical counterpart we identify a star with  $V \sim 14.6$  (Table 4) which shows a sudden brightness increase by  $\sim 0.85$  mag and  $\sim 0.6$  mag in the MACHO R- and B-band light curves. A fast decline in the OGLE I-band data after the end of the MACHO observations suggests a return to a lower brightness level (Fig. 7). Such a behaviour is seen from about 15% of the (single) Be stars in the SMC (type-2 in Mennickent et al. 2002).

## 4. Be/X-ray binaries with previously known pulse period

#### 4.1. *The 263 s Be/X-ray binary pulsar XMMU J004723.7-731226*

Haberl & Sasaki (2000) proposed RX J0047.3-7312 (= AX J0047.3-7312) as HMXB candidate due to its possible identification with the  $H\alpha$  emission line star [MA93] 172. The detection in a first XMM-Newton observation on 2000 Oct. 15 supported the optical identification (Haberl & Pietsch 2004, designated the source XMMU J004723.7-731226). A finding chart for the optical counterpart of XMMU J004723.7-731226 was published by Coe et al. (2005, SXP264 in Fig. 1), who suggested as counterpart the northern star in a crowded region with at least three stars.

Our XMM-Newton observations covered XMMU J004723.7-731226 twice. The new, astrometrically improved X-ray positions (Table 2) are not compatible with the proposed counterpart by Coe et al. (2005), but indicate the star more southwest as counterpart. This star also corresponds to the MCPS and OGLE stars listed in Table 4, while the entry from the UBV catalog does not resolve the stars. From a previous XMM-Newton observation on 2000 Oct. 15, pulsations with a period of  $263.64 \pm 0.30$  s were detected. The new measurement of  $262.23 \pm 0.66$  s in Oct. 2006 indicates a slight spin-up. In the March 2007 observation we were not able to detect any significant periodicity from XMMU J004723.7-731226 (neither in the power spectra nor by folding techniques). This may be caused by the relative noisy structure of the pulse profile (Fig. 9) in combination with background flaring activity during the observation 0403970301. The X-ray luminosities during our observations on 2006 Oct. 5 and 2007 March 12 (Table 5) were nearly identical, but almost a factor of 5 lower than on 2000 Oct. 15. The X-ray spectrum was harder when the source was brighter (photon index of  $0.76 \pm 0.04$  on 2000 Oct. 15). The deep dip in the broad band pulse profile present on 2000 October 15 (Fig. 3 of Haberl & Pietsch 2004) is no longer seen anymore on 2006 Oct. 5, but this might be caused by the lower statistics in the new observation. Overall, the pulse profiles appear highly structured (Fig. 9).

#### 4.2. *The 25.5 s Be/X-ray binary pulsar XMMU J004814.1-731003*

This pulsar was discovered in observation 0404680101 and first results were published by Haberl et al. (2008). The results from

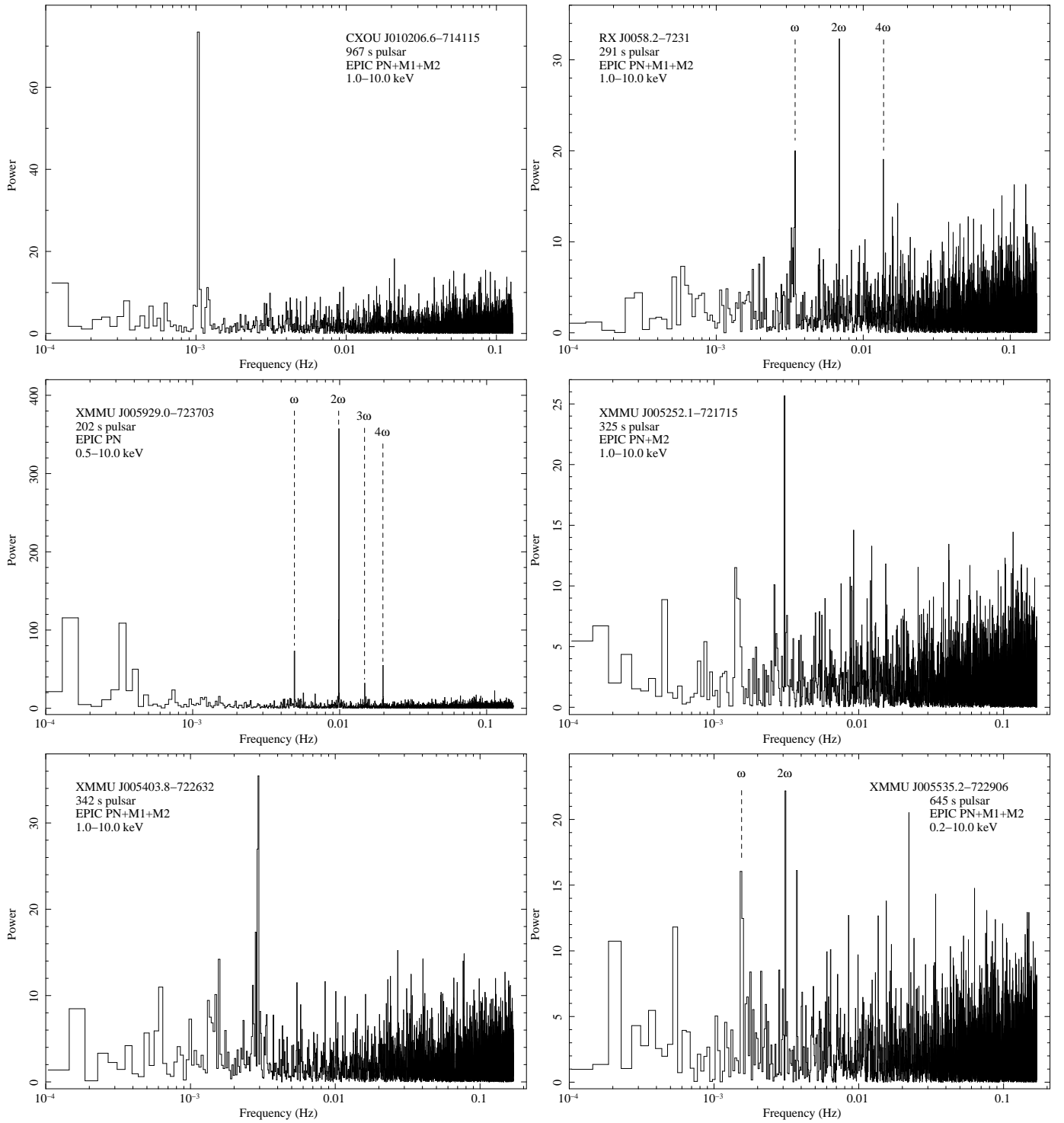


**Fig. 4.** Power spectra of newly discovered pulsars obtained from the EPIC data in broad energy bands. To improve statistics in most cases the three instruments PN, MOS1 and MOS2, when available, were combined for the timing analysis.

the spectral analysis are repeated in Table 5. XMMU J004814.1-731003 was fainter during observation 0403970301, about five months later (the data became public after the discovery paper). Scaling from the EPIC-PN 0.2–4.5 keV count rate ( $4.6 \times 10^{-2}$  cts  $s^{-1}$  compared to  $2.0 \times 10^{-3}$  cts  $s^{-1}$ ) with the assumption of constant spectral shape, the source luminosity decreased by a factor of 23. Due to the faintness of the source no pulsations were detected in the new observation.

#### 4.3. The 500 s Be/X-ray binary pulsar CXOU J005455.6-724510

The pulse period of  $503.5 \pm 6.7$  s from this pulsar was first reported by Edge et al. (2004c) from a Chandra observation on 2002, July 4. This period was confirmed by Haberl et al. (2004) from XMM-Newton data taken on 2003, Dec. 18. Pulse profiles and spectra were presented from the EPIC data and the pulse period during the XMM-Newton observation was determined to

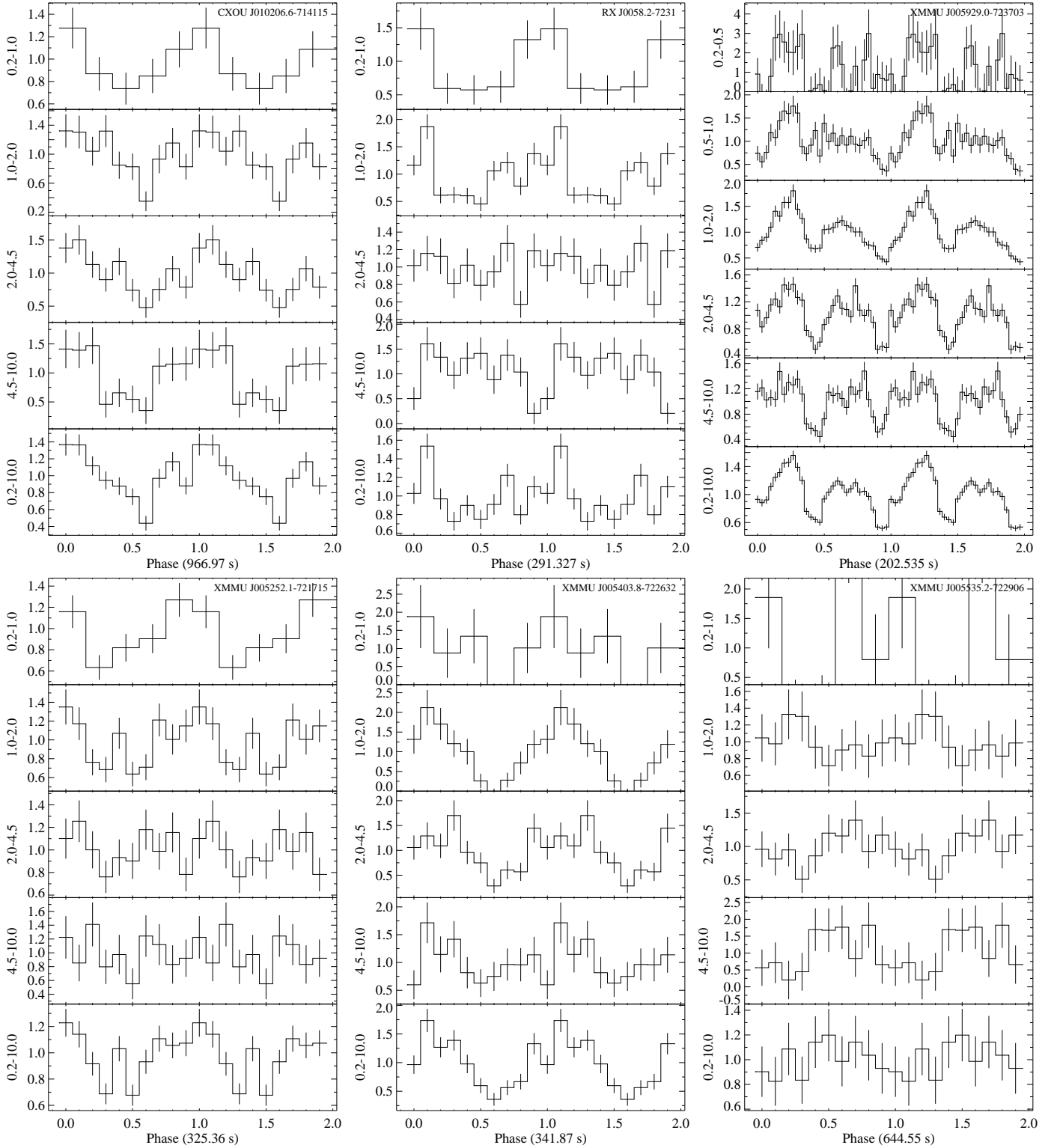


**Fig. 5.** Folded EPIC-PN light curves of newly discovered pulsars in the standard EPIC energy bands. The panels show the pulse profiles for the different energies specified in keV. The intensity profiles are background subtracted and normalised to the average count rate, as listed in Table 6.

$500.0 \pm 0.2$  s and the source luminosity to  $4 \times 10^{35}$  erg  $s^{-1}$  (0.5–10 keV).

During the new XMM-Newton observation (0404680201) in Nov. 2006, the source luminosity was somewhat lower at  $1.3 \times 10^{35}$  erg  $s^{-1}$ . The EPIC spectra are of low statistical quality. They can formally be fit with a power-law (see Table 5),

although there is indication for a soft component as seen during the first XMM-Newton observation. The pulse period has further decreased to  $497.5 \pm 1.0$ . Pulse profiles are shown in Fig. 9.

**Table 6.** Average EPIC-PN count rates of Be/X-ray binary pulsars.

Source	0.2–1.0 keV <sup>(a)</sup>	1.0–2.0 keV	2.0–4.5 keV	4.5–10.0 keV	0.2–10.0 keV
XMMU J004723.7-731226	3.6	13.5	15.5	8.6	41.1
CXOU J005455.6-724510	2.1	2.5	3.3	1.8	10.0
XMMU J004911.4-724939	1.7+6.9	53.7	79.8	62.9	206
RX J0049.7-7323	8.3	40.8	51.9	40.0	142
RX J0050.8-7316	4.8	13.2	19.3	11.0	67.8
CXOU J010712.6-723533	5.4	14.8	23.4	14.6	58.5
CXOU J010206.6-714115	10.3	12.9	15.1	8.7	47.0
XMMU J005929.0-723703	3.6+43	138	140	93	419
RX J0059.3-7223	2.4+15.3	33.5	27.1	15.8	94.4
RX J0058.2-7231	5.4	18.7	17.7	9.6	51.1
SMC X-3	8.0	21.5	26.5	15.7	73.0
XMMU J005252.1-721715	12.4	18.0	17.0	7.3	54.6
CXOU J005323.8-722715	8.0	19.5	20.2	12.4	61.4
XMMU J005403.8-722632	1.4	4.8	8.3	6.4	21.4
XMMU J005535.2-722906	–	7.8	8.7	3.5	20.1

Count rates in  $10^{-3}$  counts  $s^{-1}$  from EPIC-PN. <sup>(a)</sup> For most sources the two energy bands 0.2–0.5 keV and 0.5–1.0 keV were combined for statistical reasons. For three cases the count rates in the two bands are listed separately.

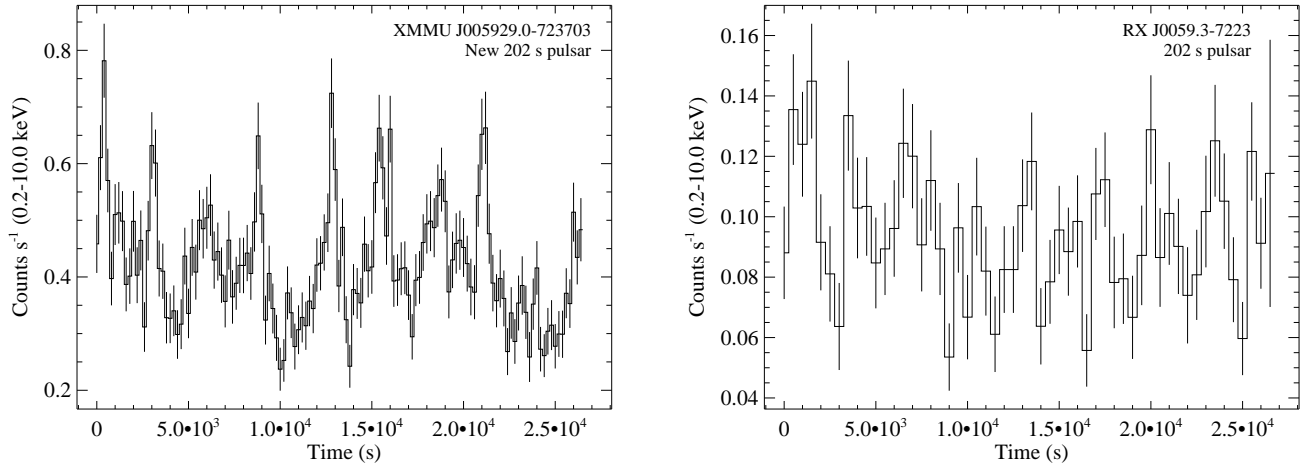


**Fig. 6.** Broad-band (0.2–10.0 keV) EPIC-PN light curves of the two 202 s pulsars observed in field 0500980201. The data is background subtracted and binned to 200 s and 500 s for XMMU J005929.0-723703 and RX J0059.3-7223, respectively. Time 0 corresponds to MJD 54257.3925.

#### 4.4. The 74.7 s Be/X-ray binary pulsar AX J0049-729

Pulsations from AX J0049-729 with a period of 74.7 s were first reported from RXTE data (Corbet et al. 1998) and then confirmed by ASCA (Yokogawa & Koyama 1998a). The identification of the ASCA source with RX J0049.1-7250 (Kahabka & Pietsch 1998) allowed the identification with a Be star (Stevens et al. 1999). Our improved X-ray position confirms object 1 in their finding chart as the correct counterpart.

AX J0049-729 was detected as faint source during observation 0403970301. The detected counts are insufficient for a spectral or temporal analysis. Adopting the same X-ray spectral shape as the nearby 18.37 s pulsar XMMU J004911.4-724939, scaling the EPIC-PN 0.2–4.5 keV count rates ( $8.8 \times 10^{-1}$  cts  $s^{-1}$  compared to  $1.8 \times 10^{-2}$  cts  $s^{-1}$ ) yields a luminosity of  $1.1 \times 10^{35}$  erg  $s^{-1}$  (Table 5).

#### 4.5. The 18.37 s Be/X-ray binary pulsar XMMU J004911.4-724939

During the XMM-Newton observation 0403970301, a bright X-ray transient, designated XMMU J004911.4-724939, was detected (Eger & Haberl 2008), only 83'' away from AX J0049-729. Our timing analysis revealed X-ray pulsations with a period of  $18.3814 \pm 0.0001$  s. The pulse period of XMMU J004911.4-724939 is consistent with that of XTE J0055-727 ( $18.37 \pm 0.01$ ; Corbet et al. 2003). This indicates, that these two sources are identical (the source position is 31' away from the RXTE pointing position, well within the PCA collimator response). The pulsar XTE J0055-727 was first detected in RXTE data (Corbet et al. 2003) when it became more active than the years before 2003 (Galache et al. 2008). Although several searches for this pulsar were performed (e.g., Haberl et al. 2004), it never was detected due to the limited FOV of the imaging instruments. The XMM-Newton position and period of XMMU J004911.4-

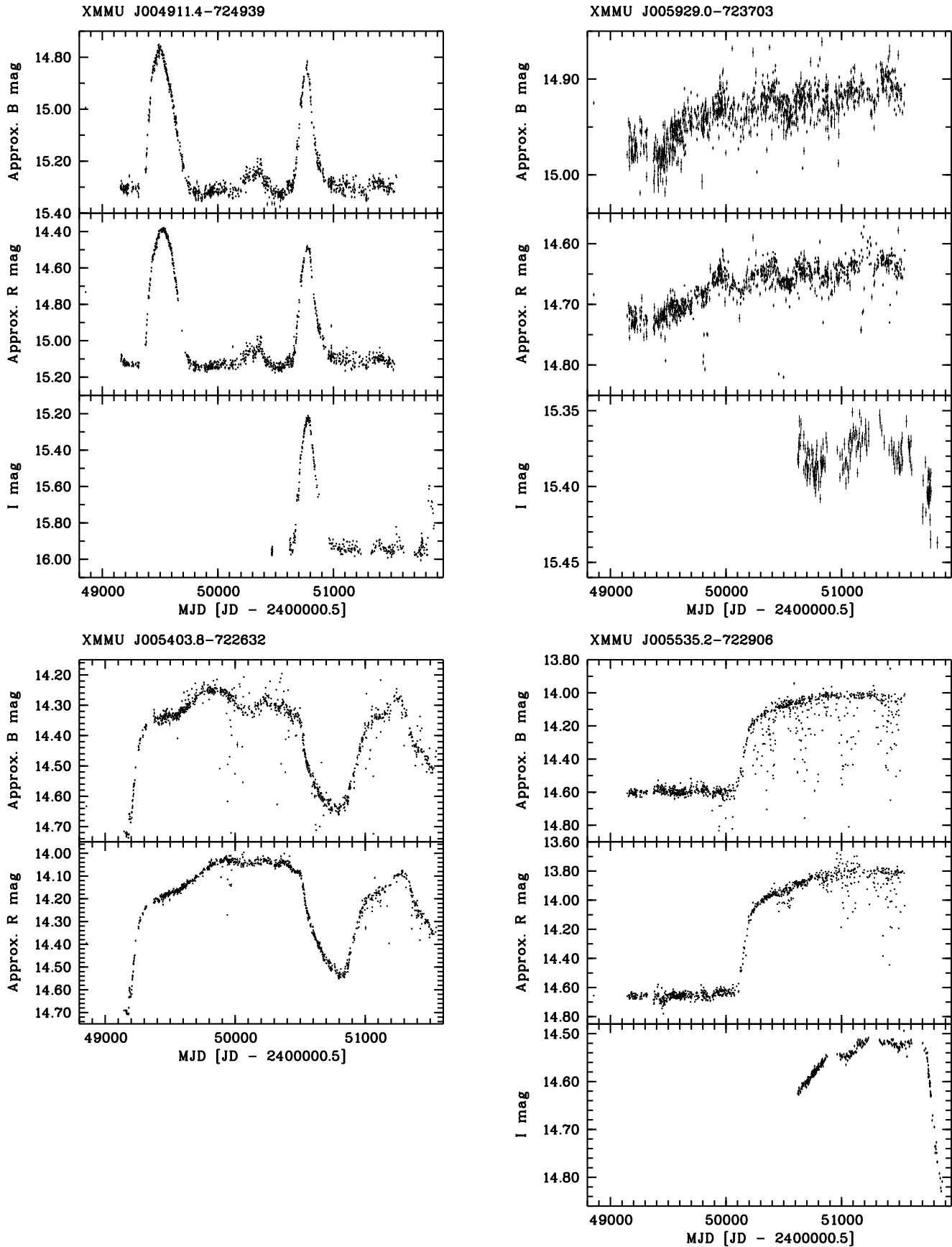


**Fig. 7.** MACHO B- and R- and OGLE I-band (when available) light curves of the optical counterparts of XMMUJ004911.4-724939 and three new Be/X-ray binary pulsars. The optical counterparts are MACHO 208.15911.13 and OGLE 65500 for XMMU J004911.4-724939, MACHO 207.16541.15 and OGLE 139407 for XMMU J005929.0-723703, MACHO 207.16202.21 for XMMU J005403.8-722632, and MACHO 207.16315.28 and OGLE 137527 for XMMU J005535.2-722906. For the MACHO data only data points with errors smaller than 0.01 mag are drawn. Large excursions in the MACHO data which are not present in the OGLE data, are probably not real.

724939 allowed us to identify a Be star as optical counterpart also for XTE J0055-727.

We show the X-ray pulse profiles in Fig. 9. No significant pulsations are seen below 0.5 keV, while at higher energies a double peaked profile (0.5-1.0 keV) develops into one with a single peak above 4.5 keV. The counting statistics is sufficient to investigate the pulse phase dependent hardness ratios (Fig. 10). The variations seen at the high energies indicate changes in the intrinsic spectrum of the source.

The EPIC pulse-phase averaged X-ray spectra are well represented by a strongly absorbed hard power-law (Table 5 and Fig. 3) with the highest luminosity in our source sample. The X-ray position allowed us to identify the pulsar with a  $V = 16.0$  mag Be star. The boresight correction applied in the current work (Table 2) brings the X-ray coordinates in full agreement with the position of the optical counterpart. We extracted MACHO and OGLE light curves which are shown in Fig. 7. Two optical outbursts, lasting about 330 and 270 days with brightness increases by  $\sim 0.55$  and  $\sim 0.50$  mag (in MACHO approximate B magnitude),  $\sim 0.8$  mag and  $\sim 0.6$  (in approximate R) for the two outbursts, respectively, and  $\sim 0.75$  mag (in OGLE I) for the second outburst. Similar behaviour is also observed from other Be stars (Mennickent et al. 2002). We conclude that XMMU J004911.4-724939 is a Be/X-ray binary pulsar in the SMC, and identical to XTE J0055-727. Coe & Udalski (2008) reported a likely orbital period of 17.8 days from OGLE III data.

#### 4.6. The 755 s Be/X-ray binary pulsar RX J0049.7-7323

Haberl & Sasaki (2000) suggested RX J0049.7-7323 as candidate Be/X-ray binary because of its possible counterpart, the emission line star [MA93] 315.  $H\alpha$  spectroscopy by Edge & Coe (2003) confirmed the Be/X-ray binary nature of RX J0049.7-7323. Pulsations with a period of  $755.5 \pm 0.6$  s were discovered from AX J0049.4-7323 in a very long ASCA observation in April 2000 (Yokogawa et al. 2000b), with RX J0049.7-7323 within the error circle of the ASCA source. From a first XMM-Newton observation Haberl & Pietsch (2004) confirmed the association between the ROSAT and the ASCA source.

We detect RX J0049.7-7323 with a pulse period of  $746.15 \pm 0.79$  s (only PN data, source on CCD boundary in MOS) confirming the strong long-term spin-up trend of this pulsar. We re-determined the period from the first XMM-Newton observation using the combined EPIC data to  $752.14 \pm 0.43$  s and show the spin period history in (Fig. 11). The period has decreased by nearly 10 s over 7.0 years resulting in an average period derivative of  $1.34 \text{ s y}^{-1}$ . Pulse profiles are shown in Fig. 9.

#### 4.7. The 323 s Be/X-ray binary pulsar RX J0050.8-7316

RX J0050.8-7316 was identified with a variable Be star ( $V \sim 15.4$ ) by Cowley et al. (1997). Two period measurements from ASCA observations were reported from AX J0051-733 Yokogawa & Koyama (1998b); Yokogawa et al. (2003), which the authors identify with the ROSAT source by positional coincidence. An accurate X-ray position and the detection of pulsations in XMM-Newton data from 2000 Oct. 15 confirmed this identification (Haberl & Pietsch 2004).

During the new XMM-Newton observation, RX J0050.8-7316 was detected with a period of  $317.44 \pm 0.26$  s continuing the spin-up seen before (Fig. 11). The average period derivative between the first ASCA and the last XMM-Newton observation is  $0.62 \text{ s y}^{-1}$ . The RXTE period measurements show a large

scatter which might partially be caused by different flux contributions of our newly discovered pulsar (Sect. 3.4) with similar period or by other nearby variable sources contributing to the X-ray flux. In Fig. 9 we present the pulse profiles which show a deep relatively narrow feature with a energy-dependent shape.

#### 4.8. The 172 s Be/X-ray binary pulsar AX J0051.6-7311

The 172 s pulsations of this source were first discovered in ASCA data (AX J0051.6-7311 = RX J0051.9-7311; Torii et al. 2000; Cowley et al. 1997). The source was right at the edge of the field of view of observation 0404680301 (Fig. 1), only marginally covered by MOS2. No sensible parameters could be derived.

#### 4.9. The 15.3 s Be/X-ray binary pulsar RX J0052.1-7319

Lamb et al. (1999) detected pulsations from RX J0052.1-7319 in ROSAT data. A faint source compatible with the position of this pulsar was detected in observation 0404680301 with an EPIC-PN 0.2–4.5 keV count rate of  $1.14 \times 10^{-2} \text{ cts s}^{-1}$  which translates into a luminosity of  $4.0 \times 10^{34} \text{ erg s}^{-1}$  (scaling to SMC X-3 with a count rate of  $1.24 \times 10^{-1} \text{ cts s}^{-1}$ , i.e. assuming a power-law spectrum with  $\gamma = 0.92$  and SMC  $N_{\text{H}} = 5 \times 10^{21} \text{ cm}^{-2}$ , justified due to the similar hardness ratios of the two sources). The collected counts were also not sufficient for a period search.

#### 4.10. The 65.8 s Be/X-ray binary pulsar CXOU J010712.6-723533

Observation 0404680501 covers only one Be/X-ray binary, the pulsar CXOU J010712.6-723533. It was discovered in the course of the SMC wing survey performed with Chandra on 2006 Feb. 10 with a period of  $65.78 \pm 0.13$  s and a luminosity of  $\sim 3 \times 10^{36} \text{ erg s}^{-1}$  (McGowan et al. 2008). During the XMM-Newton observation the source was detected as the brightest point source in the EPIC images with a luminosity of  $6.0 \times 10^{35} \text{ erg s}^{-1}$  (Table 7, see below), which is about four times fainter than during the Chandra observation. Although the absorption column density was not constrained by the Chandra spectrum, the photon indices suggest a harder spectrum during the Chandra observation with higher X-ray luminosity. From the EPIC data (2007 April 12) we determined the pulse period to  $65.94 \pm 0.02$  s, within the errors consistent with the Chandra measurement. The pulse profiles (Fig. 9) are dominated by a broad peak.

The EPIC spectra of CXOU J010712.6-723533 are not well modelled by a simple power-law as the reduced  $\chi^2$  indicates (the worst of our power-law model fits, Table 5). Systematic residuals (Fig. 3), similar to those observed from the 6.85 s pulsar XTE J0103-728 in the SMC (Haberl & Pietsch 2008b) or, e.g., the Be/X-ray binary X Persei in the Milky Way (La Palombara & Mereghetti 2007), indicate excess emission on top of the power-law. Adding a blackbody component yields similar properties as those found for X Persei. We summarise characteristic parameters obtained from this model in Table 7 and show the EPIC spectra with best fit model in Fig. 8.

#### 4.11. The 565 s Be/X-ray binary pulsar CXOU J005736.2-721934 = XMMU J005735.7-721932

This long-period pulsar was independently found as Be/X-ray binary in XMM-Newton and Chandra observations. XMM-Newton observed it on 2000 October 17 and 2002 March 30 (in

the same field as the 202 s pulsar RX J0059.3-7223, see next section). Sasaki et al. (2003) suggested the emission line star [MA93] 1020 as optical counterpart. The source was faint with  $4.1 \times 10^{34}$  erg s<sup>-1</sup> and  $8.2 \times 10^{33}$  erg s<sup>-1</sup>, respectively. From a 100 ks Chandra observation on 2001 May 15, Macomb et al. (2003) reported the detection of the pulse period of  $564.8 \pm 0.4$  s and a source luminosity of  $6.2 \times 10^{34}$  erg s<sup>-1</sup> (for 60 kpc). The Chandra position was also consistent with the position of [MA93] 1020. H $\alpha$  spectroscopy of the optical counterpart revealed a complicated profile of the H $\alpha$  line with four peaks (Coe et al. 2005) which the authors interpret as the start of a new period of mass ejection from the Be star.

During our new XMM-Newton observation a source was detected right at the edge of the EPIC-PN field of view (not covered by EPIC-MOS1) at a position compatible with that of the pulsar. There are too few counts for a temporal and spectral analysis.

#### 4.12. The 202 s Be/X-ray binary pulsar RX J0059.3-7223

The ROSAT source RX J0059.3-7223 was first classified as X-ray binary candidate by Kahabka et al. (1999) using hardness ratio criteria. It was observed twice by XMM-Newton on 2000 October 17 and 2002 March 30 (Sasaki et al. 2003). X-ray pulsations of  $201.9 \pm 0.5$  s were detected in the EPIC-MOS data of the October 2000 observation, when the source was observed at a large off-axis angle with the MOS detectors while it was outside the EPIC-PN field of view (Majid et al. 2004). Significant modulation in the X-ray flux was mainly detected at energies above 2 keV. During the 2002 March observation the source flux was 70% of that of the earlier observation and the period was determined to  $201.2 \pm 0.5$  s (Majid et al. 2004). The proposed optical counterpart (see also Table 4) was investigated by Coe et al. (2005). These authors presented the MACHO and OGLE light curves in the V- and I-band, respectively, which show very high optical variability, but no significant optical periodicity. The X-ray and optical data clearly identify this source as Be/X-ray binary pulsar.

During our new XMM-Newton observation RX J0059.3-7223 was the second-brightest source in the field with about a factor of five lower count rate as XMMU J005929.0-723703, the other new 202 s pulsar. The light curve shows flaring variability by a factor of about two, but the lower statistics requires longer time binning and the flares can not be fully resolved (Fig. 6). Timing analysis yields a pulse period of  $200.50 \pm 0.29$  s which may indicate a slight spin-up trend over 6.7 years, but the periods measured at the three epochs are still compatible within their  $2\sigma$  uncertainties. Pulse profiles and hardness ratios were derived and are shown in Figs. 9 and 10. The pulse profiles show little variation below  $\sim 2$  keV as seen before (Majid et al. 2004) and a broad pulse with a sharp drop on top of a flat light curve for energies between 2.0 and 4.5 keV. At higher energies the pulse seems to be smeared out to a more sinusoidal profile. Pulse-phase averaged spectra were accumulated and are well reproduced by the power-law model with parameters typical for Be/X-ray binaries in the SMC (Table 5, Fig. 3).

#### 4.13. The 7.78 s Be/X-ray binary pulsar SMC X-3

SMC X-3 was originally detected by Clark et al. (1978) in SAS 3 data during a strong X-ray outburst with  $7 \times 10^{37}$  erg s<sup>-1</sup>. Only recently it was identified with a previously detected 7.78 s RXTE pulsar by using archival Chandra data (Edge et al. 2004a). During the RXTE monitoring of the SMC a spin-down trend in

the pulse period of SMC X-3 is seen to around 7.79 s by the end of 2005 (Galache et al. 2008). We detected SMC X-3 with a pulse period of  $7.7912 \pm 0.0096$  s consistent with this development. The X-ray luminosity (Table 5) was more than a factor of six lower than during the the Chandra observation on 2002 July 20 (Edge et al. 2004b), when the source also showed a harder spectrum. The XMM-Newton EPIC energy resolved pulse profiles (Fig. 9) show a relatively smooth, broad peak at energies below 1 keV, but indicate a highly structured shape at energies above 1 keV.

As in the case of CXOU J010712.6-723533 the power-law model fit to the EPIC spectra of SMC X-3 yields a relatively bad reduced  $\chi^2$  and similarly structured residuals (Fig. 3). Adding a blackbody component improves the fit considerably (Table 7, Fig. 8). Similar parameters for the blackbody components from the two pulsars are inferred.

#### 4.14. The 138 s Be/X-ray binary pulsar CXOU J005323.8-722715

This pulsar was discovered in a Chandra observation on 2002 July 20 (Edge et al. 2004b) with a period of  $138.04 \pm 0.61$  s (98% confidence). We confirm this source as pulsar and determined the period to  $139.136 \pm 0.016$  s from the XMM-Newton observation on 2007 June 23, indicating significant spin-down of the neutron star. We present the pulse profiles of CXOU J005323.8-722715 in Fig. 9 showing a broad, single peak in all EPIC energy bands similar to that seen in the broad band Chandra data, but with much increased statistical quality.

#### 4.15. The 59 s Be/X-ray binary pulsar XTE J0055-724

The pulse period of this source was discovered in RXTE data (Marshall & Lochner 1998) and subsequent observations with BeppoSAX refined the pulse period to  $58.969 \pm 0.001$  s and the positional uncertainty to a radius of  $50''$  (Santangelo et al. 1998). This uncertainty was further reduced to  $10''$  by the identification of XTE J0055-724 = 1SAX J0054.9-7226 with RX J0054.9-7226 (Israel 1998) which led to the identification of the optical counterpart (Stevens et al. 1999). No broad band X-ray spectrum could be obtained yet. Also in the EPIC data, XTE J0055-724 was detected only as weak source with just too few counts for spectral fitting (spectral parameters are largely unconstrained). The 0.2–4.5 keV count rate of  $2.67 \times 10^{-2}$  cts s<sup>-1</sup> from the EPIC-PN camera translates into a luminosity of  $9.2 \times 10^{34}$  erg s<sup>-1</sup> (scaling to the nearby 138 s pulsar CXOU J005323.8-722715 with a count rate of  $8.70 \times 10^{-2}$  cts s<sup>-1</sup>, i.e. assuming a power-law spectrum with  $\gamma = 0.97$  and SMC  $N_{\text{H}} = 2.9 \times 10^{21}$  cm<sup>-2</sup> which is justified by very similar hardness ratios of the two sources). A pulse period search around the expected value yielded a period of  $58.858 \pm 0.001$  s, i.e. a net spin-up of 0.11 s over the 9.4 years between the BeppoSAX and XMM-Newton observations.

## 5. Be/X-ray binaries without detected X-ray pulsations

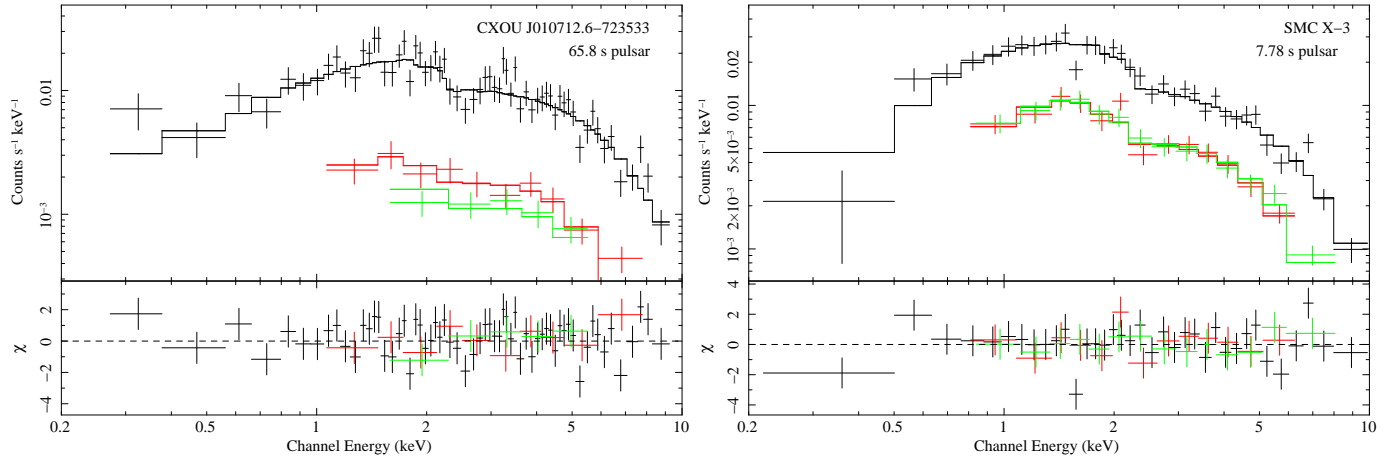
#### 5.1. The Be/X-ray binary RX J0048.5-7302

This ROSAT source was proposed as candidate Be/X-ray binary by Haberl & Sasaki (2000) due to its identification with the H $\alpha$  emission line star [MA93] 238. From a first XMM-Newton observation Haberl & Pietsch (2004) reported an improved X-ray position which supported the optical identification. The first

**Table 7.** Spectral fit results for a power-law component with additional blackbody emission.

Source	SMC $N_{\text{H}}$ [ $10^{21} \text{ cm}^{-2}$ ]	Photon Index	kT keV	Radius km	Flux <sup>(a)</sup> erg $\text{cm}^{-2} \text{ s}^{-1}$	$L_{\text{x}}^{(b)}$ erg $\text{s}^{-1}$	$\chi^2/\text{dof}$
CXOU J010712.6-723533	<1.5	0.23±0.23	1.3±0.2	0.74	$1.4 \times 10^{-12}$	$6.0 \times 10^{35}$	1.17/71
SMC X-3	$2.0^{+1.6}_{-1.0}$	0.79±0.07	$1.1^{+0.3}_{-0.2}$	0.73	$8.5 \times 10^{-13}$	$3.8 \times 10^{35}$	0.98/56

(<sup>a</sup>) Observed 0.2-10.0 keV flux. (<sup>b</sup>) Source intrinsic X-ray luminosity in the 0.2-10.0 keV band (corrected for absorption) for a distance to the SMC of 60 kpc (Hilditch et al. 2005).

**Fig. 8.** EPIC spectra of two Be/X-ray binaries which are not well modelled by a power-law (see Fig. 3). Including a hot blackbody component to the model yields acceptable fits.

EPIC spectra were also consistent with a power-law with a spectral index of 0.9, typical for HMXBs. The optical counterpart was covered by the 2dF survey of the SMC and Evans et al. (2004) obtained a spectral type of B0-5(II), strongly suggesting RX J0048.5-7302 as Be/X-ray binary.

Our boresight corrected X-ray position from the new XMM-Newton observation on 2007 March 12 is within  $0.2''$  consistent with the optical counterpart, fully confirming the association. The source was detected with an EPIC-PN count rate of  $3.1 \times 10^{-3} \text{ cts s}^{-1}$ , not sufficient for spectral or for timing analysis. On 2000 Oct. 15 the count rate was  $2.7 \times 10^{-2} \text{ cts s}^{-1}$ , a factor of 8.5 higher. Scaling the X-ray luminosity given in Haberl & Pietsch (2004) by this factor (adjusting the distance to 60 kpc) yields the value given in Table 5.

### 5.2. The Be/X-ray binaries RX J0049.2-7311 and RX J0049.5-7310

These two ROSAT sources with an angular distance of  $80''$  were both discussed as possible counterparts of the ASCA 9.13 s pulsar AX J0049-732 (Yokogawa et al. 2003). RX J0049.5-7310 was proposed as candidate Be/X-ray binary by Haberl & Sasaki (2000) due to its identification with the  $H\alpha$  emission line star [MA93] 300 and therefore favoured as counterpart to AX J0049-732 by Filipović et al. (2000). Later, also for RX J0049.2-7311 a  $H\alpha$  emission line star was found as optical counterpart (Coe et al. 2005, Table 4) and because the position of RX J0049.2-7311 is formally closer to the best ASCA position of AX J0049-732 these authors preferred this as more likely identification. However, due to the relatively wide point spread function of the ASCA telescope the extraction radius of  $3'$  used for the analysis of AX J0049-732 (Yokogawa et al. 2000a) en-

compasses both ROSAT sources and a secure identification of AX J0049-732 with either of the ROSAT sources can only be made through the detection of pulsations.

RX J0049.2-7311 and RX J0049.5-7310 were both detected in the XMM-Newton observation 0404680101 in Oct. 2006 at a similar X-ray luminosity (Table 5). Their X-ray spectra are typical for HMXBs and given their optical counterparts, which are both consistent with Be stars, they are clear cases of Be/X-ray binaries in the SMC. Both sources were also detected in a previous XMM-Newton observation in Oct. 2000 (Haberl & Pietsch 2004). While RX J0049.2-7311 was at the same brightness level, RX J0049.5-7310 was almost a factor of 4 fainter during the earlier XMM-Newton observation. No significant pulsations were detected in the range between 0.2 s and 2000 s in the EPIC data of either observation. The non-detection of 9.13 s pulsations might even suggest, that none of the two ROSAT sources is the counterpart of the ASCA source.

During the April 2007 observation RX J0049.5-7310 was not detected. RX J0049.2-7311 was again at a similar brightness level as seen by XMM-Newton before. Scaling from the PN 0.2–4.5 keV count rate (0404680101:  $5.0 \times 10^{-2} \text{ cts s}^{-1}$  compared to 0403970301:  $6.6 \times 10^{-2} \text{ cts s}^{-1}$ ) with the assumption of a constant spectral shape, the source luminosity of RX J0049.2-7311 increased slightly by a factor of 1.3 from Oct. 2006 to March 2007 (Table 5).

Despite the non-detection of any significant periodicity from either of the two sources, we confirm both as Be/X-ray binaries from their optical counterpart and their X-ray spectral properties.

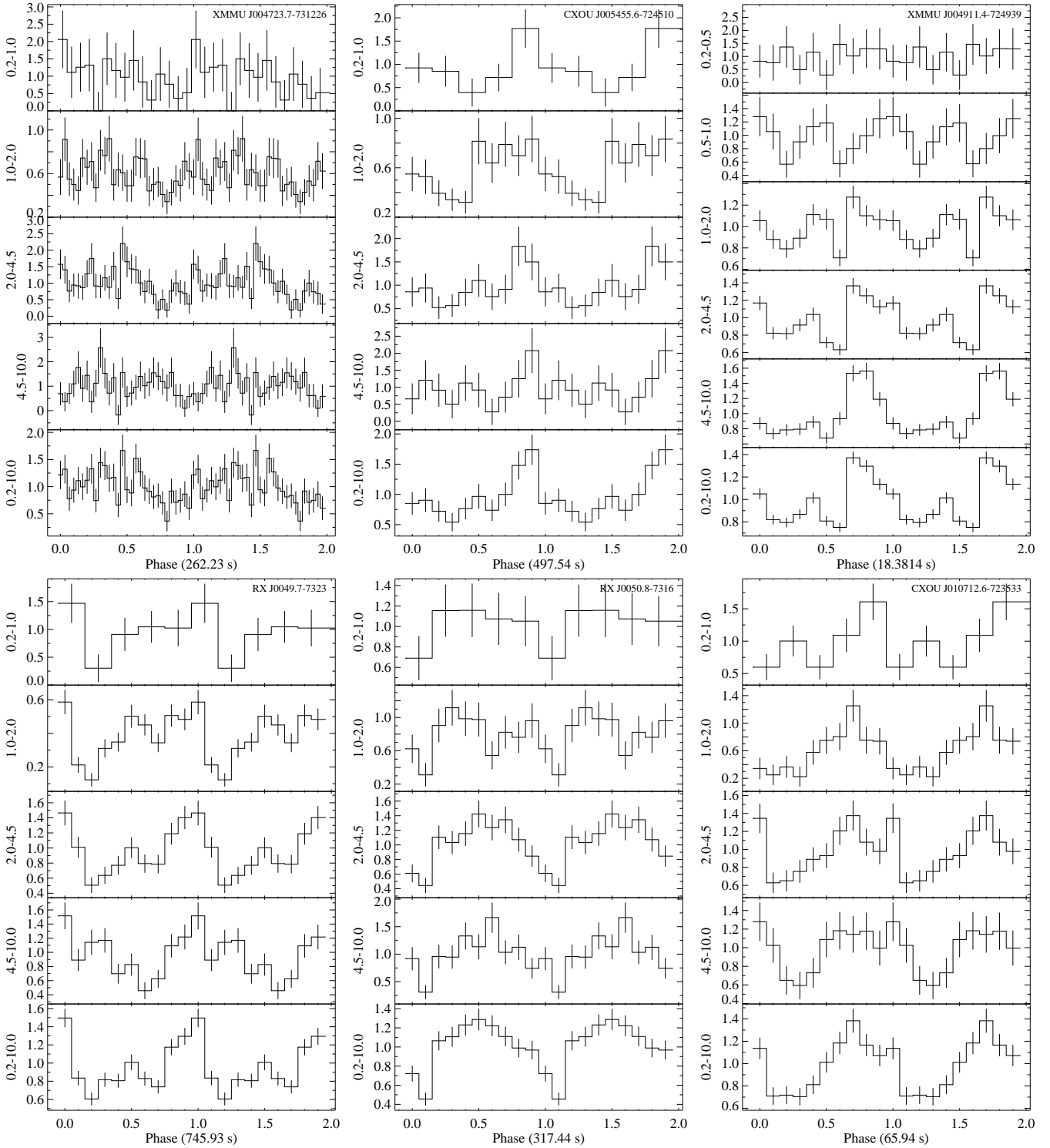


**Fig. 9.** Folded EPIC-PN light of Be/X-ray binaries with previously identified pulse periods. Presentation as in Fig. 5.

### 5.3. The Be/X-ray binary RXJ0049.5-7331

RXJ0049.5-7331 is another candidate Be/X-ray binary proposed by Haberl & Sasaki (2000) due to its likely identification with the  $H\alpha$  emission line star [MA93] 302. The X-ray position obtained from the EPIC images (within  $0.17''$  of the optical position from MCPS, Table 4) further supports this identification. The DSS2 red image shows a pair of close bright stars with similar brightness and colours which is not resolved in the UBV $R$  catalogue entry. The X-ray position is consistent with the north-

ern of the two stars. The X-ray spectrum of RXJ0049.5-7331 (Table 5) indicates a relatively hard power-law with little absorption in the SMC in addition to the Galactic foreground column density. The EPIC X-ray spectrum and its optical counterpart clearly identify RXJ0049.5-7331 as Be/X-ray binary in the SMC.

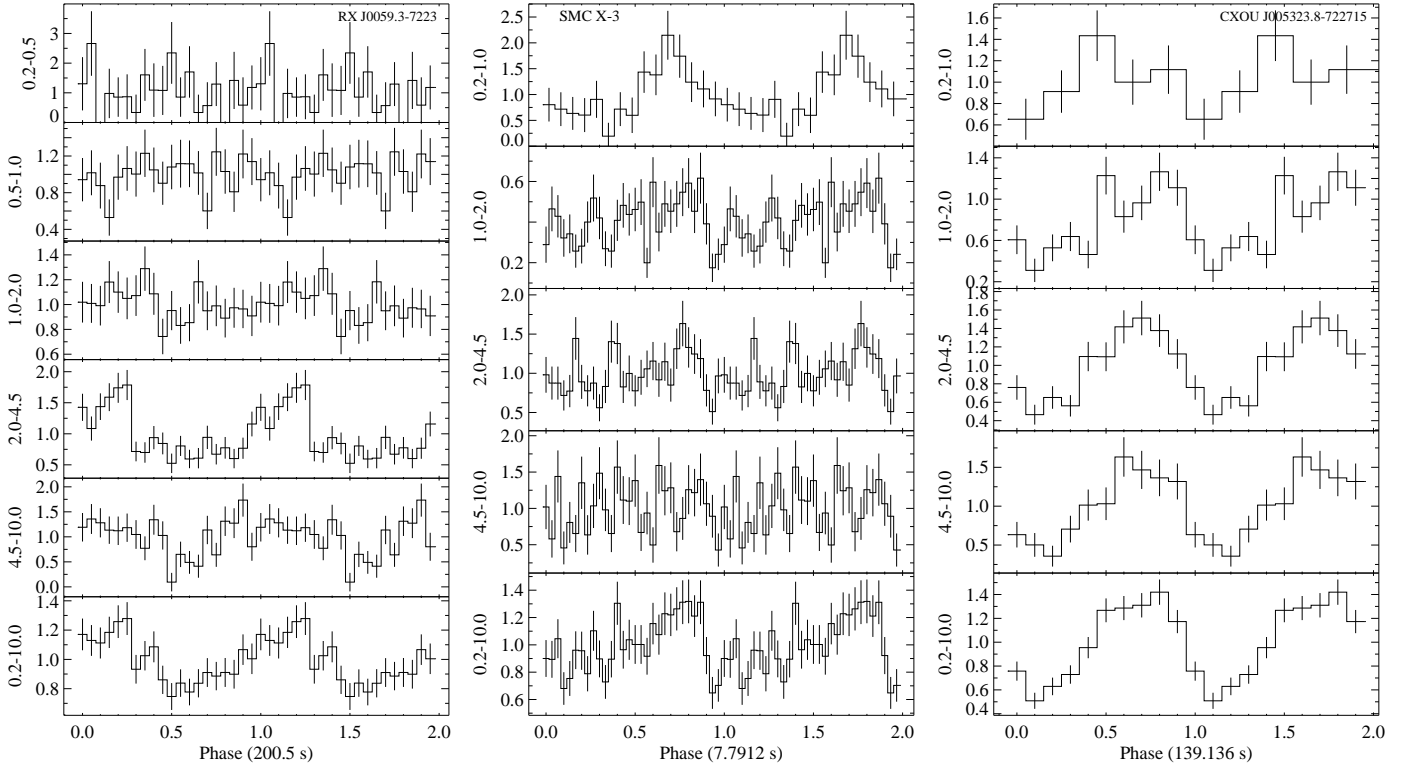


**Fig. 9.** Continued

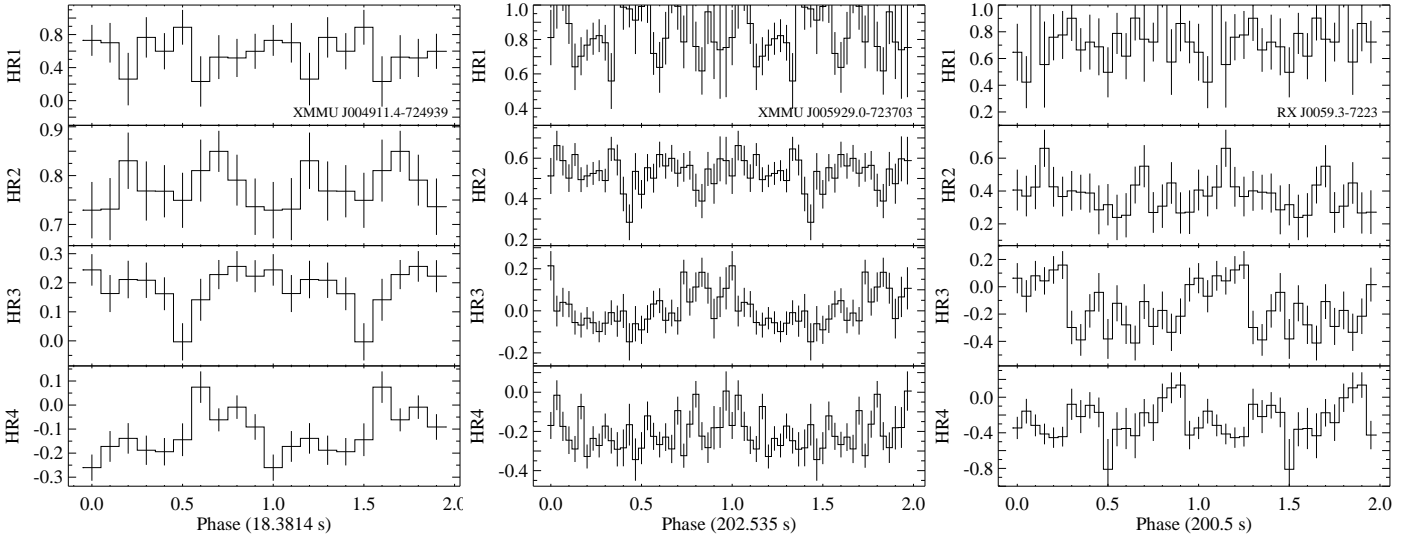


**Fig. 10.** Hardness ratios HR1, HR2, HR3 and HR4 as function of pulse phase of three Be/X-ray pulsars, derived from their folded EPIC-PN light curves shown in Figs. 5 and 9. The 18.37 s pulsar XMMU J004911.4-724939 was observed in field 0403970301 while the two pulsars XMMU J005929.0-723703 and RX J0059.3-7223 with periods close to 202 s are both located in field 0500980201.

#### 5.4. The Be/X-ray binary RX J0101.8-7223

This source was detected in ROSAT PSPC (source 220 in the catalogue of Haberl et al. 2000) and HRI (source 97; Sasaki et al. 2000) pointed observations. Haberl & Sasaki (2000) suggested it as Be/X-ray binary candidate because of a possible identification with the  $H\alpha$  emission line object [MA93] 1288. However, this needed confirmation due to the relatively large ROSAT position error of  $\sim 8''$ . Our improved XMM-Newton position (within  $1.3''$  of the optical position of [MA93] 1288 from MCPS, Table 4)

supports the identification with the emission line star. The star was included in the 2dF survey of the SMC and Evans et al. (2004) infer a spectral type of B0-5(II).

No X-ray pulsations have been detected so far from this Be/X-ray binary. We also did not detect any significant periodic signal in the EPIC data between 0.2 s and 2000 s. The EPIC spectra are consistent with an absorbed power-law with typical values for  $N_{\text{H}}$  and photon index (Table 5) for Be/X-ray binaries.

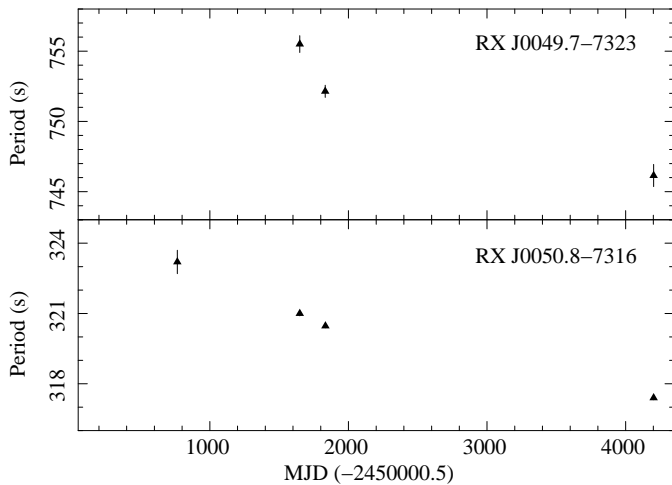


**Fig. 11.** Spin period history of two SMC pulsars covered by our observations. The first measurement for RX J0049.7-7323 (= AX J0049.4-7323, see Sect. 4.6) and the first two measurements for RX J0050.8-7316 (= AX J0051-733, see Sect. 4.7) were reported from ASCA data (Yokogawa et al. 2000b, 2003, respectively). The last two data points for each pulsar are derived from XMM-Newton observations.

The X-ray and optical properties point to the identification of RX J0101.8-7223 as a Be/X-ray binary.

## 6. Discussion and conclusions

We detected a large sample of twenty-six Be/X-ray binaries in eight XMM-Newton observations of the SMC between Oct. 2006 and June 2007. After astrometric boresight corrections the accurate X-ray positions allowed us either to confirm previously proposed optical counterparts or, in cases of the newly discovered systems, to identify their counterparts. The properties of all optical counterparts (like brightness, colours and long-term temporal behaviour) are consistent with Be/X-ray binaries. No candidate for a supergiant HMXB was found.

Twenty of the sources were observed with luminosities above  $\sim 10^{35}$  erg s $^{-1}$ , providing X-ray spectra and light curves for a detailed, systematic study. Most of the X-ray spectra can be modelled by an absorbed power-law, typical for HMXBs. The average power-law index is 0.93 with 90% of the values between 0.71 and 1.27, which is in agreement with the peak of the distribution at 1.0 found by Haberl & Pietsch (2004) for a smaller sample. McGowan et al. (2007) report harder spectra from four Be/X-ray binary pulsars detected in the Chandra SMC wing survey and discuss possibilities for systematic differences between pulsars in the wing and the bar of the SMC. We see a general trend of harder power-law spectra when the sources are brighter (e.g. XMMU J004723.7-731226, Sect. 4.1; CXOU J010712.6-723533, Sect. 4.10) which suggests that the harder spectra in the wing pulsars might at least partly be due to a brightness selection effect. From the short ( $\sim 10$  ks) Chandra observations, spectra could only be derived when the sources were bright.

The highest luminosities were reached by the 18.37 s pulsar XMMU J004911.4-724939 and the new 202 s pulsar XMMU J005929.0-723703 with  $5.5 \times 10^{36}$  erg s $^{-1}$  and  $4.5 \times 10^{36}$  erg s $^{-1}$ , respectively, while all other sources with EPIC spectra were observed with luminosities between  $10^{35}$  erg s $^{-1}$  and  $10^{36}$  erg s $^{-1}$ . Six Be/X-ray binaries were detected only as faint sources (for four of them we estimate their luminosity from the

count rates, the other two are located at the edge of the field of view) and about 5-10 Be/X-ray binaries (uncertain positions and unclear classifications make the numbers uncertain) were not detected in our eight fields. I.e. we now know about 31-36 Be/X-ray binaries in the eight fields from which 26 (about 70-85%) are detected above a luminosity of  $4 \times 10^{34}$  erg s $^{-1}$  (the weakest detected sources have count rates down to  $1 \times 10^{-3}$  cts s $^{-1}$  for EPIC-PN which converts to  $4 \times 10^{33}$  erg s $^{-1}$  for a typical HMXB power-law spectrum).

For twelve of the Be/X-ray binaries covered by our XMM-Newton observations, orbital ephemeris obtained from RXTE X-ray data are available (Galache et al. 2008). All our clear detections are from orbital phases near zero (which defines maximum X-ray intensity as seen by RXTE). Consistently, three pulsars observed around phase 0.4 were found to be either faint or not detected. The 74.7 s pulsar AX J0049-729, the 59 s pulsar XTE J0055-724 and the 82.4 s pulsar XTE J0052-725 were relatively faint during the XMM-Newton observations close to phase 0, but the uncertainties in their ephemeris do not allow an exact determination of the orbital phase. Therefore, it is not clear if the outbursts were missed by the XMM-Newton observations or if they did not happen. Overall, the luminosity states in which we found the Be/X-ray binaries during the XMM-Newton observations are all consistent with the orbital variations determined by RXTE. This also suggests, that we did not observe any type II outburst with XMM-Newton.

Systematic deviations from the power-law model are seen in the spectra of a few of our investigated Be/X-ray binaries (Fig. 3). In particular CXOU J010712.6-723533 and SMC X-3 yield bad power-law fits (in terms of reduced  $\chi^2$  as can be seen from Table 5). Additional cases might be RX J0050.8-7316 and XMMU J005252.1-721715. However, spectra with better statistical quality are required to prove this. Expanding the model with a blackbody component yields acceptable fits for CXOU J010712.6-723533 and SMC X-3. The inferred blackbody temperatures are around 1.2 keV and the sizes of the emitting areas are relatively small (radius  $\sim 0.7$  km). These spectral characteristics are similar to those of RX J0146.9+6121 and X Persei (La Palombara & Mereghetti 2006, 2007). These authors interpret the blackbody component as emission from the hot polar caps of the accreting neutron star (for a discussion of the origin of soft emission excesses see Hickox et al. 2004).

We discovered X-ray pulsations from four new transient Be/X-ray binaries (for the 325 s pulsar XMMU J005252.1-721715 an independent discovery from Chandra data was reported by Coe et al. 2008) and found pulsations from two previously known Be/X-ray binaries. The pulse periods range between 202 s and 967 s, the latter being the second longest known from SMC pulsars. The high statistical quality of the EPIC data allowed us to investigate pulse profiles in several different energy bands, revealing a large variety of pulse shapes and different energy dependence.

All of our investigated pulsars with pulse periods longer than 150 s and known period history over at least a few years show secular spin-up of the neutron star. They all exhibit more or less regular outburst activity as seen by RXTE (Galache et al. 2008). At shorter spin periods at least two of the pulsars show long-term spin-down: the 138 s pulsar CXOU J005323.8-722715, which was detected only twice by RXTE at high brightness level (Galache et al. 2008) and the 7.78 s pulsar SMC X-3. The periods determined for the 18.37 s pulsar XMMU J004911.4-724939 are consistent with no change. This fits in the general picture of the spin evolution of accretion powered pulsars, in which the neutron star is spun-up by accretion until an equilibrium period

is reached (see, e.g. equations 8 and 9 in Bildsten et al. 1997). The fact that the majority of long-period pulsars in the SMC show secular spin-up, suggests however a much longer timescale for spinning up the neutron star, as was also seen for HMXB pulsars in the Milky Way. High resolution BATSE measurements of the long-term spin evolution of HMXB pulsars have shown that the small long-term spin-up rates are a consequence of frequent transitions between spin-up and spin-down which can occur on timescales of less than 10 days (Bildsten et al. 1997). To confirm such a behaviour for SMC Be/X-ray binary pulsars would require a monitoring program with XMM-Newton with frequent observations for several weeks.

With the new discoveries, we now know of several pairs of SMC pulsars with very similar periods. In particular two 202 s pulsars exist with an angular distance of only  $13.8'$ . RX J0059.3-7223 was discovered with a period of  $201.9 \pm 0.5$  s in October 2000, which decreased to  $200.5 \pm 0.3$  s, and XMMU J005929.0-723703 was discovered with  $202.52 \pm 0.02$  s. A similar case is XMMU J005403.8-722632, newly discovered in this work with a period of  $341.87 \pm 0.15$  s, and SAX J0103.2-7209 with the earliest measured period of  $348.9 \pm 0.1$  s (in ASCA data from May 1996; Yokogawa & Koyama 1998c), which decreased to  $341.2 \pm 0.5$  s in October 2000 (Haberl & Pietsch 2004). These two pulsars are located  $45.2'$  apart. Due to the overlapping ranges of spin periods which evolve with time and the projected proximity of many Be/X-ray binaries in the SMC some of these pulsar pairs may not be differentiated by non-imaging instruments which needs to be considered when interpreting the spin period evolution.

The SMC absorption component varies over a wide range between a few  $10^{20}$   $\text{cm}^{-2}$  and several  $10^{22}$   $\text{cm}^{-2}$ . It is evident, that the sources in field 0500980101 show similar values of low absorption, while those of field 0404680101, near the emission nebula N19, show all very high absorption. For further investigation we list the total HI column density of the SMC in the direction of each source in the last column of Table 5. In Fig. 12 the X-ray measured column density  $N_{\text{H}}$  is plotted as functions of the B-V colour index of its optical counterpart (from MCPS in Table 4) and the total SMC column density as derived from HI measurements. In both cases a correlation is indicated, although with considerable scatter in  $N_{\text{H}}$ . The scatter is expected as 1) the sources are located at different depth in the SMC and 2) a large part of the absorption can originate locally in the Be/X-ray binary systems (suggested by strong variations of  $N_{\text{H}}$  over longterm timescales as seen, e.g., from RX J0103.6-7201; Haberl & Pietsch 2005). The general increase of the X-ray measured  $N_{\text{H}}$  with the total SMC column density suggests that a significant fraction of the X-ray absorption seen in the X-ray spectra of Be/X-ray binaries arises in the interstellar medium of the SMC.

*Acknowledgements.* The XMM-Newton project is supported by the Bundesministerium für Wirtschaft und Technologie/Deutsches Zentrum für Luft- und Raumfahrt (BMWi/DLR, FKZ 50 OX 0001) and the Max-Planck Society. The ‘‘Second Epoch Survey’’ of the southern sky was produced by the Anglo-Australian Observatory (AAO) using the UK Schmidt Telescope. Plates from this survey have been digitised and compressed by the ST ScI. Produced under Contract No. NAS 5-26555 with the National Aeronautics and Space Administration. This paper utilises public domain data obtained by the MACHO Project, jointly funded by the US Department of Energy through the University of California, Lawrence Livermore National Laboratory under contract No. W-7405-Eng-48, by the National Science Foundation through the Center for Particle Astrophysics of the University of California under cooperative agreement AST-8809616, and by the Mount Stromlo and Siding Spring Observatory, part of the Australian National University.

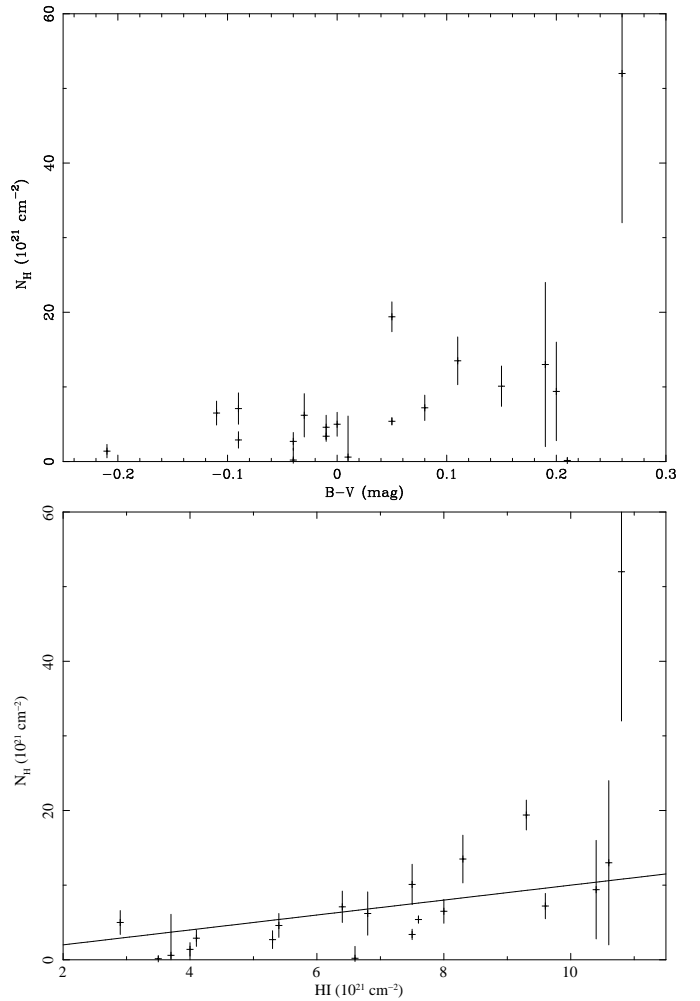


**Fig. 12.** Equivalent hydrogen column density derived from the X-ray spectra as a function of the optical colour index B-V (top) and as a function of the total HI column density of the SMC. The line in the bottom panel marks  $N_{\text{H}} = \text{HI}$ .

## References

- Bildsten, L., Chakrabarty, D., Chiu, J., et al. 1997, *ApJS*, 113, 367  
 Clark, G., Doxsey, R., Li, F., Jernigan, J. G., & van Paradijs, J. 1978, *ApJ*, 221, L37  
 Coe, M. J., Edge, W. R. T., Galache, J. L., & McBride, V. A. 2005, *MNRAS*, 356, 502  
 Coe, M. J., Schurch, M., Corbet, R. H. D., et al. 2008, *MNRAS* in press, *ArXiv e-prints* 0803.3941  
 Coe, M. J. & Udalski, A. 2008, *The Astronomer’s Telegram*, 1458, 1  
 Corbet, R., Markwardt, C. B., Marshall, F. E., Laycock, S., & Coe, M. 2002, *IAU Circ.*, 7932, 2  
 Corbet, R., Marshall, F. E., Lochner, J. C., Ozaki, M., & Ueda, Y. 1998, *IAU Circ.*, 6803, 1  
 Corbet, R. H. D., Markwardt, C. B., Coe, M. J., et al. 2003, *The Astronomer’s Telegram*, 214, 1  
 Corbet, R. H. D., Markwardt, C. B., Coe, M. J., et al. 2004, *The Astronomer’s Telegram*, 273, 1  
 Cowley, A. P., Schmidtke, P. C., McGrath, T. K., et al. 1997, *PASP*, 109, 21  
 Edge, W. R. T. & Coe, M. J. 2003, *MNRAS*, 338, 428  
 Edge, W. R. T., Coe, M. J., Corbet, R. H. D., et al. 2004a, *The Astronomer’s Telegram*, 225, 1  
 Edge, W. R. T., Coe, M. J., Galache, J. L., et al. 2004b, *MNRAS*, 353, 1286  
 Edge, W. R. T., Coe, M. J., & McBride, V. A. 2004c, *The Astronomer’s Telegram*, 217, 1  
 Eger, P. & Haberl, F. 2008, *The Astronomer’s Telegram*, 1453, 1  
 Evans, C. J., Howarth, I. D., Irwin, M. J., Burnley, A. W., & Harries, T. J. 2004, *MNRAS*, 353, 601  
 Filipović, M. D., Haberl, F., Winkler, P. F., et al. 2008, *A&A* in press

- Filipović, M. D., Pietsch, W., & Haberl, F. 2000, *A&A*, 361, 823
- Galache, J. L., Corbet, R. H. D., Coe, M. J., et al. 2008, *ApJS* in press, ArXiv e-prints 0802.2118
- Gregory, P. C. & Loredano, T. J. 1996, *ApJ*, 473, 1059
- Haberl, F., Eger, P., Pietsch, W., Corbet, R. H. D., & Sasaki, M. 2008, *A&A* in press, ArXiv e-prints 0803.2473
- Haberl, F., Filipović, M. D., Pietsch, W., & Kahabka, P. 2000, *A&AS*, 142, 41
- Haberl, F. & Pietsch, W. 2004, *A&A*, 414, 667
- Haberl, F. & Pietsch, W. 2005, *A&A*, 438, 211
- Haberl, F. & Pietsch, W. 2008a, in *X-rays from Nearby Galaxies*, MPE Report 295, 32 (ArXiv e-prints 0712.2720)
- Haberl, F. & Pietsch, W. 2008b, *A&A* in press, ArXiv e-prints 0801.4679
- Haberl, F., Pietsch, W., Schartel, N., Rodriguez, P., & Corbet, R. H. D. 2004, *A&A*, 420, L19
- Haberl, F. & Sasaki, M. 2000, *A&A*, 359, 573
- Hickox, R. C., Narayan, R., & Kallman, T. R. 2004, *ApJ*, 614, 881
- Hilditch, R. W., Howarth, I. D., & Harries, T. J. 2005, *MNRAS*, 357, 304
- Hughes, J. P. 1994, *ApJ*, 427, L25
- Israel, G. L. 1998, *IAU Circ.*, 6822, 2
- Israel, G. L., Stella, L., Angelini, L., et al. 1997, *ApJ*, 484, L141
- Israel, G. L., Stella, L., Campana, S., et al. 1998, *IAU Circ.*, 6999, 1
- Jansen, F., Lumb, D., Altieri, B., et al. 2001, *A&A*, 365, L1
- Kahabka, P. & Haberl, F. 2006, *A&A*, 452, 431
- Kahabka, P. & Pietsch, W. 1998, *IAU Circ.*, 6840, 1
- Kahabka, P., Pietsch, W., Filipović, M. D., & Haberl, F. 1999, *A&AS*, 136, 81
- La Palombara, N. & Mereghetti, S. 2006, *A&A*, 455, 283
- La Palombara, N. & Mereghetti, S. 2007, *A&A*, 474, 137
- Lamb, R. C., Prince, T. A., Macomb, D. J., & Finger, M. H. 1999, *IAU Circ.*, 7081, 4
- Laycock, S., Corbet, R. H. D., Coe, M. J., et al. 2003, *MNRAS*, 339, 435
- Lomb, N. R. 1976, *Ap&SS*, 39, 447
- Macomb, D. J., Fox, D. W., Lamb, R. C., & Prince, T. A. 2003, *ApJ*, 584, L79
- Majid, W. A., Lamb, R. C., & Macomb, D. J. 2004, *ApJ*, 609, 133
- Marshall, F. E. & Lochner, J. C. 1998, *IAU Circ.*, 6818, 1
- Massey, P. 2002, *ApJS*, 141, 81
- McBride, V. A., Coe, M. J., Bird, A. J., et al. 2007, *MNRAS*, 382, 743
- McGowan, K. E., Coe, M. J., Schurch, M., et al. 2007, *MNRAS*, 376, 759
- McGowan, K. E., Coe, M. J., Schurch, M. P. E., et al. 2008, *MNRAS*, 383, 330
- Mennickent, R. E., Cidale, L., Pietrzyński, G., Gieren, W., & Sabogal, B. 2006, *A&A*, 457, 949
- Mennickent, R. E., Pietrzyński, G., Gieren, W., & Szewczyk, O. 2002, *A&A*, 393, 887
- Meyssonnier, N. & Azzopardi, M. 1993, *A&AS*, 102, 451
- Okazaki, A. T. & Negueruela, I. 2001, *A&A*, 377, 161
- Russell, S. C. & Dopita, M. A. 1992, *ApJ*, 384, 508
- Santangelo, A., Cusumano, G., Israel, G. L., et al. 1998, *IAU Circ.*, 6818, 1
- Sasaki, M., Haberl, F., & Pietsch, W. 2000, *A&AS*, 147, 75
- Sasaki, M., Pietsch, W., & Haberl, F. 2003, *A&A*, 403, 901
- Scargle, J. D. 1982, *ApJ*, 263, 835
- Schmidtke, P. C., Cowley, A. P., Crane, J. D., et al. 1999, *AJ*, 117, 927
- Shtykovskiy, P. & Gilfanov, M. 2005, *MNRAS*, 362, 879
- Stanimirovic, S., Staveley-Smith, L., Dickey, J. M., Sault, R. J., & Snowden, S. L. 1999, *MNRAS*, 302, 417
- Stevens, J. B., Coe, M. J., & Buckley, D. A. H. 1999, *MNRAS*, 309, 421
- Strüder, L., Briel, U., Dennerl, K., et al. 2001, *A&A*, 365, L18
- Szymanski, M. K. 2005, *Acta Astronomica*, 55, 43
- Torii, K., Yokogawa, J., Imanishi, K., & Koyama, K. 2000, *IAU Circ.*, 7428, 3
- Turner, M. J. L., Abbey, A., Arnaud, M., et al. 2001, *A&A*, 365, L27
- Udalski, A., Kubiak, M., & Szymanski, M. 1997, *Acta Astronomica*, 47, 319
- Udalski, A., Szymanski, M., Kubiak, M., et al. 1998, *Acta Astronomica*, 48, 147
- Wilms, J., Allen, A., & McCray, R. 2000, *ApJ*, 542, 914
- Yokogawa, J., Imanishi, K., Tsujimoto, M., Koyama, K., & Nishiuchi, M. 2003, *PASJ*, 55, 161
- Yokogawa, J., Imanishi, K., Tsujimoto, M., et al. 2000a, *ApJS*, 128, 491
- Yokogawa, J., Imanishi, K., Ueno, M., & Koyama, K. 2000b, *PASJ*, 52, L73
- Yokogawa, J. & Koyama, K. 1998a, *IAU Circ.*, 6835, 2
- Yokogawa, J. & Koyama, K. 1998b, *IAU Circ.*, 6853, 2
- Yokogawa, J. & Koyama, K. 1998c, *IAU Circ.*, 7009, 3
- Zaritsky, D., Harris, J., Thompson, I. B., Grebel, E. K., & Massey, P. 2002, *AJ*, 123, 855
- Zavlin, V. E., Pavlov, G. G., Sanwal, D., & Trümper, J. 2000, *ApJ*, 540, L25